

# Structural evolution and sediment depositional system along the transform margin- Palar–Pennar basin, Indian east coast

Swagato Dasgupta<sup>a</sup>, Mery Biswas<sup>b</sup>, Soumyajit Mukherjee<sup>c,\*</sup>, Rima Chatterjee<sup>a</sup>

<sup>a</sup> Department of Applied Geophysics, Indian Institute of Technology (ISM) Dhanbad, India

<sup>b</sup> Department of Geography, Presidency University, Kolkata, India

<sup>c</sup> Department of Earth Sciences, Indian Institute of Technology Bombay, Mumbai, 400 076, Maharashtra, India

## ARTICLE INFO

### Keywords:

Tectonics  
Sedimentation  
Stratigraphy  
Geomorphology  
Pull-apart basin  
Chronostratigraphy

## ABSTRACT

Continental transform margins are characterized by sub-vertical strike-slip faults and rapid change in thermal gradient across the margin from continental to oceanic crust. The continental crust terminates abruptly along such sheared margins. Tectonic evolution associated with sedimentation in continental slope of the Palar–Pennar transform margin is inadequately understood due to limited seismic data and/or poor imaging with few well controls. Exploratory drilling attempts for hydrocarbon presence have resulted in some promising outcomes in the Palar–Pennar basin.

The Palar–Pennar graben in onland is bound by steep normal rift faults, which reactivated by strike-slip movement during late syn-rift time as Antarctica separated along the NNW to ~ N-trending Coromandal transform margin in the offshore part. The pre-existing Precambrian shear zones and lineaments in the basement have played a governing role in the basin development. The onland drainage pattern is structurally controlled as observed from its rectangular drainage pattern, tectonic index and sinuosity index. In offshore area of the basin, seismic interpretation identifies distinct pull-apart rift basin along the Coromandal transform margin with syn-rift deposits in the lower continental slope portion. Strike-slip movement uplifted the fault blocks in the southern part of the pull-apart basin. This has also reactivated some of the rift faults in the syn-rift section. Such reactivation results in early post-rift seal breach. This tectonic event has implication in the depositional sequences, which has been portrayed by seismic stratigraphic analysis and construction of chronostratigraphic section across the transform margin in this work. Thickening of post-rift deposition towards E–SE, major hiatus, large scale mass transport complexes and erosional events have been identified from such analysis. On this basis, seven distinct tectonic sequences, M1 to M5 in Mesozoic and T1 and T2 in Tertiary, have been identified. The chronostratigraphic section can help in deciphering the relative sea level changes based on the nature of stratal terminations, extent of erosion and non-deposition. This study emphasizes the tectonic-controlled drainage system and geometry as well as sedimentation pattern in onland and offshore deepwater area of Palar – Pennar basin alongside the Coromandal transform margin.

## 1. Introduction

Study of sheared continental margins/transform margins is of global interest, for both academicians as well as petroleum geoscientists. Transform margins generally have narrow shelf – slope system with steep continental slope as a result of high-angle strike-slip faulting associated with a thinned lithosphere (Basile et al., 1998; Nemčok et al., 2016; Misra and Dasgupta, 2018a). Tectonic activities (thermal uplifts and subsidence) along a transform margin is expected to impact the offshore sedimentation pattern (Basile et al., 1993, 1998, 2012; Watts,

2001; Antobreh et al., 2009; Nemčok et al., 2016). Seismic stratigraphic study across such pull-apart basins adjacent to transform margin helps to understand the stratigraphic architecture based upon the stratal terminations.

The Palar–Pennar basin initiated during the Permo-Triassic rifting, resembling the Pranhita-Godavari rift system, having a N to NNE basinal trend situated in southern part of the peninsular India, north of the Cauvery basin (Fig. 1A, Rangaraju et al., 1993; Sastri et al., 1973; Bastia and Radhakrishna, 2012). Later, it formed a part of a peri-cratonic rift system of the Indian peninsula as the Indian plate broke apart from the

\* Corresponding author.

E-mail addresses: [soumyajitm@gmail.com](mailto:soumyajitm@gmail.com), [smukherjee@iitb.ac.in](mailto:smukherjee@iitb.ac.in) (S. Mukherjee).

<https://doi.org/10.1016/j.petrol.2022.110155>

Received 22 June 2021; Received in revised form 24 November 2021; Accepted 10 January 2022

Available online 14 January 2022

0920-4105/© 2022 Elsevier B.V. All rights reserved.

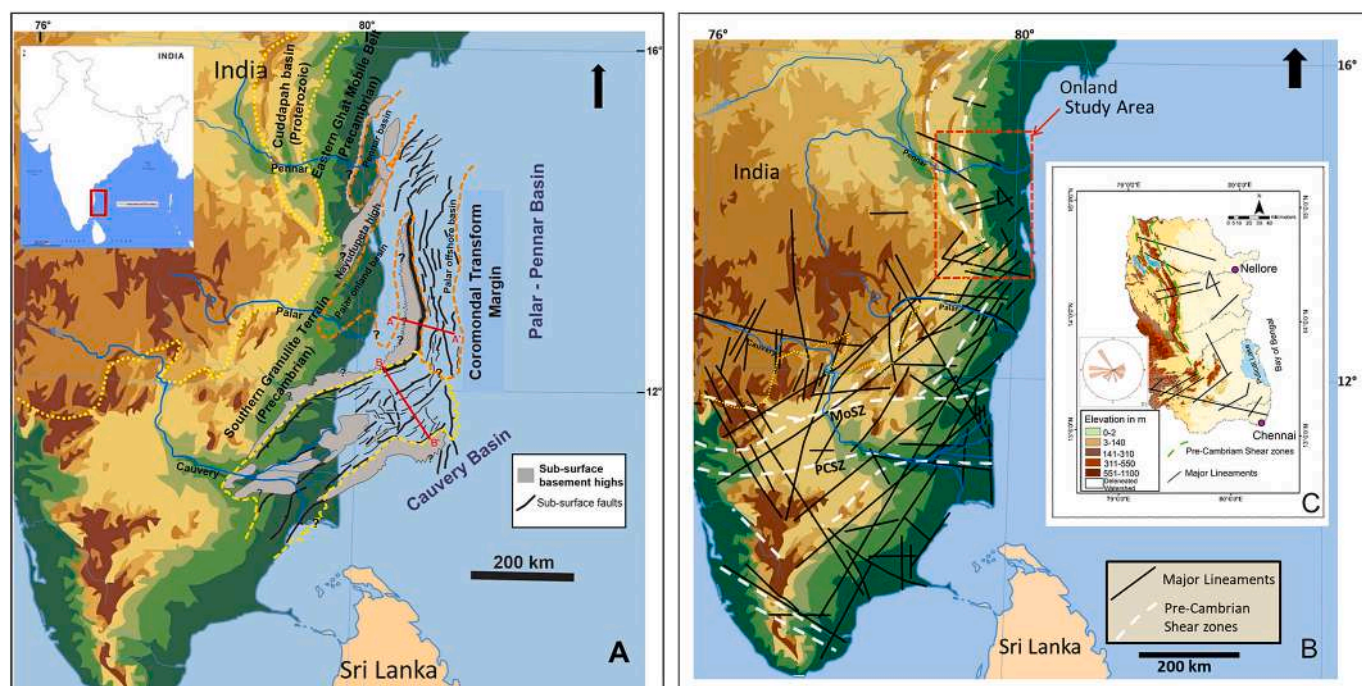


**Fig. 1.** (A) Tectonic map of Cauvery – Palar–Pennar region depicting the rift faults and the Coromondal transform margin that are overlaid on the physiographic map of India. AA': seismo-geological (Fig. 2) and chronostratigraphic sections (Fig. 4) across the Palar offshore pull-apart basin. BB': chronostratigraphic section (Fig. 12) across the Cauvery offshore basin. Dashed yellow lines on the physiographic map of India: Precambrian basin/area boundaries. Inset map: location in the Indian east coast (modified from Bastia et al., 2010; Nemčok et al., 2013a; Dasgupta, 2019). (B) Lineaments and Precambrian shear zones map of south Indian peninsular comprising of Cauvery – Palar–Pennar region (compiled and modified from Burke and Sengor, 1989; Varadarajan and Ganju, 1989; Mahadevan, 1994; Dasgupta, 2000; Mahadevan, 2003; Gopalakrishnan, 2003; Ramakrishnan, 2003; Subrahmanyam et al., 2006; Ramasamy et al., 2011; Tripathy et al., 2019). Red box: onland study area, MoSZ - Moyal Shear Zone, PCSZ - Palghat Cauvery Shear Zone. Also see Achyuthan and Thirunavukarasu (2009) for local maps. (C) Elevation profile map of the onland study area between Nellore and Chennai overlaid with tectonic lineaments. (C1) Rose diagram showing the trend of the lineaments from the study area. (For interpretation of the references to colour in this figure legend, the reader is referred to the Web version of this article.)

Antarctica during Early Cretaceous (Lal et al., 2009; Bastia et al., 2010). The Palar basin, characterized by ~ NE-trending rift faults with half-graben morphology, extends into the deep-water continental slope area of the present day Bay of Bengal. On the other hand, the Pennar graben, also known as Pulicat depression, is mostly restricted in the onland to shallow water part (Vairavan, 1993; Rangaraju et al., 1993; Mazumder et al., 2018).

In terms of hydrocarbon prospectivity, the Palar - Pennar basin has been considered as Type II, Category I basin, i.e. 'poor potential high risk basin' (Bhoj, 2008; Biswas, 2012; Dwivedi, 2016; URL-2). In past decade gas condensate discovery was made in post-rift Late Cretaceous clastic reservoir in deep water area of southern Palar basin (URL 1,2). Hydrocarbon shows were also recorded from synrift clastic reservoirs in offshore grabens in the northern part of the basin (Saxena et al., 2012; Dave et al., 2013). This clearly suggests that more studies are much required in this basin to ascertain the hydrocarbon prospectivity and to delineate the risk and uncertainties.

The Palar - Pennar basin evolved similar to that of the Cauvery basin towards south and the Krishna-Godavari (K-G) basin in the north during Mid-Late Jurassic to Early Cretaceous with NE to NNE-trending faults (Sastri et al., 1973; Biswas et al., 1993; Bastia and Radhakrishna, 2012; Nemčok et al., 2013a, b). However, subsequent to the rift stage the major displacement shifted along the NNW cross faults orthogonal to the Cauvery and the K-G rift system that extended into a dextral strike-slip transform margin, along which Antarctica and subsequently the Elan Bank micro-continental plate separated from the Indian plate ~120 Ma (Veevers and Tewari, 1995; Borissova et al., 2003; Veevers, 2009; Krishna et al., 2009; Nemčok et al., 2013a; Dasgupta, 2019). This NNW-trending dextral strike-slip transfer zone, comprising of a horse-tail structure, is known as the Coromondal transform margin,

which extends for ~200–300 km (Fig. 1A; Sinha et al., 2010; Nemčok et al., 2013a, b; Misra and Dasgupta, 2018a; Dasgupta, 2019). These tectonic movements during Mesozoic produced a pull-apart basin in offshore deep water Palar - Pennar basin alongside the Coromondal transform margin (Lal et al., 2009; Bastia et al., 2010; Nemčok et al., 2013a; Misra and Dasgupta, 2018a; Dasgupta, 2018a), having a maximum width of ~44 km (Nemčok et al., 2013a) at the central part.

During Permo-Triassic rifting, deposition of Lower Gondwana Talchir-equivalent sediments occurred in both Palar and Pennar onland grabens as inferred from field exposures and drilled well data (Rangaraju et al., 1993; Mazumder et al., 2013; Dasgupta, 2021). In the later part during Late Jurassic to Early Cretaceous, uplift of the Nayudupeta ridge separated both these basins (Fig. 1; Vairavan, 1993; Rangaraju et al., 1993; Bastia and Radhakrishna, 2012). This uplift is characterized by deposition of the Sripurumbudur Formation (Supplementary Table 1).

The entire study area (Fig. 1A and B) that includes both onshore and offshore regions, witnessed different tectonic events from Proterozoic to Tertiary (Vairavan, 1993; Nemčok et al., 2013a, b; Mazumder et al., 2018) and is even neo-tectonically active (Resmi et al., 2016, 2019; Susanth et al., 2021a, b). These events governed the paths and gradients of various present day rivers and streams (Fig. 1B and C) in the onland area. The tectonic intricacy is characterized by the developed watersheds over the area. Geologically, the deformation of the area initiated during the convergence between the proto East Antarctica block and proto Indian shield in Precambrian (Naqvi and Rogers, 1987; Mezger and Cosca, 1999; Boger et al., 2000, 2001; Carson et al., 2000; Powell and Pisarevsky, 2002; Tripathy and Saha, 2013; Mukherjee et al., 2019), which generated the basement fabric of the basin. These Precambrian basement structural fabrics further guided the subsequent rifting events

**Table 1**  
Details of applied linear and special scale methods for analysing tectonic signatures.

<u>Sl. No.</u>	<u>Indices</u>	<u>Relief Characterizes</u>	<u>Reference</u>
1.	Relative Relief	$R_R = H_R - L_R$ H <sub>R</sub> – Highest Relief L <sub>R</sub> – Lowest Relief	Smith (1935)
2.	Gradient Map	Extracted from DEM in Arc GIS10.3	NA
3.	Aspect Map	Extracted from DEM in Arc GIS10.3	NA
<u>Sl. No.</u>	<u>Indices</u>	<u>Drainage Analysis</u>	<u>Reference</u>
1.	Drainage Density	$D_d = L_u/A$ (Extracted from DEM in Arc GIS10.3.) L <sub>u</sub> – Total stream length, A-Total area	Horton (1945)
2.	Stream Order	Hierarchic order.	Strahler (1952); Rai et al. (2017)
3.	Drainage Pattern	Extracted from Drainage map and plotted in Hillshade.	Morisawa (1985)
<u>Sl. No.</u>	<u>Indices</u>	<u>Morphometric Parameters</u>	<u>Reference</u>
1.	Normalize long profile	The linear function $y = ax + b$ The logarithmic function $y = a \ln x + b$ Where, y is the elevation (H/H <sub>0</sub> ; H = elevation of each point, H <sub>0</sub> = elevation of the source), x is the length of the river (L/L <sub>0</sub> ; L = distance of the point from the source, L <sub>0</sub> = total length of the stream), a and b are the coefficients derived independently from each profile. The R2 value determines the best fit. The curve with Highest R2 value is the best-fit curve. (Extracted from SRTM 30 m DEM and formulated using Arc GIS 10.4 and TNT mips 2014 platform)	e.g. Lee and Tsai (2009); Kale et al. (2014); Paul and Biswas (2019)
2.	Concavity Index(Θ)	$C_{eh} = \frac{1}{S_2 - S_1} \Delta E$ Where, S <sub>1</sub> is the channel slope prior to disturbance, S <sub>2</sub> is the channel slope after disturbance (e.g. due to a change in incision rate E) and ΔE is the difference between the incision rate before and after disturbance.	e.g. Wobus et al. (2006); Whipple et al. (2007)
3.	Stream Gradient Index (SL)	$SL = \frac{f}{\ln D_2 - \ln D_1}$ Where, f = fall in elevation (e <sub>2</sub> -e <sub>1</sub> ) ln = Natural logarithm of the cumulative distance *Higher SL value indicated tectonic control over stream.	Hack (1957)
4.	Hypsometric Integral (HI)	$HI = \frac{(H_{mean} - H_{min})}{(H_{max} - H_{min})}$ Where, H mean = Mean elevation of the basin, Hmin = Minimum elevation of the basin, Hmax = Maximum elevation of the basin. HI value ≤ 0.30 states tectonically stable basin and ≥ 0.30 indicated tectonically unstable basin.	Strahler (1952); Schumm (1956); Andreani et al. (2014)
5.	Transverse topographic symmetry factor (T)	$T = \frac{D_a}{D_d}$ D <sub>a</sub> = distance between the midline of the drainage basin and the active meander belt midline and D <sub>d</sub> = distance between the midline and the basin divide. If the river flows through the midway of the basin, the resulting (T) would be '0' indicates symmetric basin. If the value is > 0, the river basin is asymmetric.	Sajadian et al. (2015); Takiéh et al. (2015)
6.	Sinuosity Index (SI)	$SI = \frac{\text{Channel Length}}{\text{Valley length}}$ Straight channel values < 1.05 Straight to Sinuous values between >1.05 and <1.50 Meandering channel indicates	Brice (1964); Schumm and Khan (1972); Miall (1977); Biswas and Dhara, (2019)

(continued on next page)

Table 1 (continued)

Sl. No.	Indices	Relief Characterizes	Reference
7.	Basin shape Index ( $B_s$ )	<p>&gt;1.50 mouth.</p> $B_s = \frac{B_l}{B_w}$ <p>Where, <math>B_l</math> = Length of the basin and <math>B_w</math> = Width of the basin measured at its widest part.</p> <p>Greater the <math>B_s</math> value, more tectonically active is the basin representing its elongated shape. Lower the <math>B_s</math> value, lesser the basin is tectonically active representing the circulatory shape.</p>	Bull and McFadden (1977); Ramírez-Herrera (1998)
8.a	Basin Perimeter,	Computed by Arc GIS software	NA
8.b	Basin Area,	10.3.1 using SRTM data 30 m.	
8.c	Basin Length.		
9.	Elongation Ratio (Re)	$Re = 2 / Lb * (A / \pi) 0.5$ <p>Where, Lb = Length of the river basin</p> <p>A = Area of the river basin</p> <ul style="list-style-type: none"> <li>• Circular (0.9-0.10), oval (0.8-0.9), less elongated (0.7-0.8), elongated (0.5-0.7), and more elongated (&lt;0.5).</li> <li>• 0.9-1.0 Circular</li> <li>0.8-0.9 Oval</li> <li>0.7-0.8 Less elongated</li> <li>&lt;0.7 Elongated</li> </ul>	Schumm (1956)  Pareta and Pareta (2011) Rai et al. (2017)

during Permo – Triassic and Mesozoic and played a major role in propagating rift faults and fragmenting continents (Krishna et al., 2009; Bastia et al., 2010; Mazumder et al., 2013, 2018, 2019).

The objective of this study is to understand the structural evolution and sedimentation pattern in the Palar–Pennar basin, specifically in the offshore part along the strike-slip margin. The tectonic activities, thermal uplifts and subsidence, along a transform margin presumably impact the offshore sedimentation pattern (Basile et al., 1993, 1998, 2012; Watts, 2001; Antobreh et al., 2009; Nemcok et al., 2016). Seismic stratigraphic study across such pull-apart basin adjacent to transform margin, will thus explain the stratigraphic architecture based upon the stratal terminations. The sediment input in the Palar – Pennar basin is dominantly controlled by (proto) Palar and Penner rivers along with their tributaries. It is quite obvious that the tectonic imprints should also exist in the onland part of the basin and for this we also studied the geomorphic constraints and drainage patterns in the onland area of the basin.

The Pennar river is situated in the north whereas the Palar river is towards south of the Palar–Pennar basin. All these rivers and streams have their sources in the western Precambrian highlands and get drained into the Bay of Bengal. A number of studies have been done in the Palar river basin area, south of Chennai (Resmi et al., 2016, 2019; Resmi and Achyuthan, 2018) related to neotectonic activities and drainage patterns. However, geomorphic study in Pennar and adjacent river basin areas is still inadequate. In the context of onland geomorphic study, we have analysed channel/basin geometry based on drainage anomalies and re-evaluate tectonic activeness, in the Nellore-Chennai intermediate onland section (Fig. 1B and C) drained by the Pennar river and other secondary streams.

## 2. Geological settings

There are only few literatures published on Palar–Pennar basin, commonly on onland and shallow water part due to limited data availability (e.g., Rangaraju et al., 1993; Rajanikanth et al., 2010; Bastia and Radhakrishna, 2012; Twinkle et al., 2016; Mazumder et al., 2013, 2018). The Pennar graben trends ~ NNE and is bound by steep basin margin faults in NW and S, while relatively gentler faults towards the

eastern margin. The maximum total sediment thickness is ~6 km with major portion comprising of syn-rift sediments (Vairavan, 1993; Saxena et al., 2012). The Pennar basin is mostly restricted in onland to some part of shallow water area, whereas the Palar basin extends in offshore with ~33,000 km<sup>2</sup> areas within 200 m bathymetry and exceeds to 95,000 km<sup>2</sup> area in deep-waters. Beyond this the basin merges with the abyssal plain of the Bay of Bengal (Rangaraju et al., 1993; Bastia and Radhakrishna, 2012; Saxena et al., 2012; Twinkle et al., 2016). During the Tertiary Period, the shelf-slope system was well established along the east coast margin (Sinha et al., 2010; Bastia and Radhakrishna, 2012). The width of the shelf is narrow (~15–30 km) along the transform margin (Faruque et al., 2014; Dar et al., 2015).

The stratigraphy of the onland Palar–Pennar basin (Supplementary Table 1; Rangaraju et al., 1993; Vaidyanadhan and Ramakrishnan, 2008; Bastia and Radhakrishna, 2012; Saxena et al., 2012; Chakraborty et al., 2012) is summarized below. The Ongul Formation is the oldest lithologic unit deposited during Permo-Triassic Period in a fluvio-glacial environment with restricted marine influence at the lower part. The Jurassic – Early Cretaceous rifting which led to India – Antarctica separation, generated a pull-apart kind of sub-basins in this area – onland as well as in offshore part. Coarser sandstone and siltstone with some interbedded carbonaceous shale deposited in a fluvio-lacustrine environment during this time (~150–130 Ma). This is known as Sriperambudur Formation in Palar basin and as the Bapatla Sandstone in the northern Pennar basin.

In 2014, an exploratory well was drilled near Chennai up to ~2400 m depth to estimate the hydrocarbon potential in the onland Palar basin (URL-3; Basavaraju et al., 2016). No hydrocarbon was reported but the well derived lithologic and biostratigraphic data indicating the presence of thick Middle – Late Jurassic interval, which has been described as a separate Formation. However, this has been doubted (Supplementary Table 2; Basavaraju et al., 2016; Govindan, 2017). Towards the end of rifting, Satyavedu Formation comprising of ferruginous sandstone, interbedded with siltstone and carbonaceous shale deposited in the Palar basin (Barremian to Aptian/Albian) in a transgressive environment. An equivalent unit in Pennar basin is known as the Pennar shale and the Krishna Formation. During late post-rift drift phase, the Palar basin (onland and shallow water area) suffered basinal uplift. This resulted in

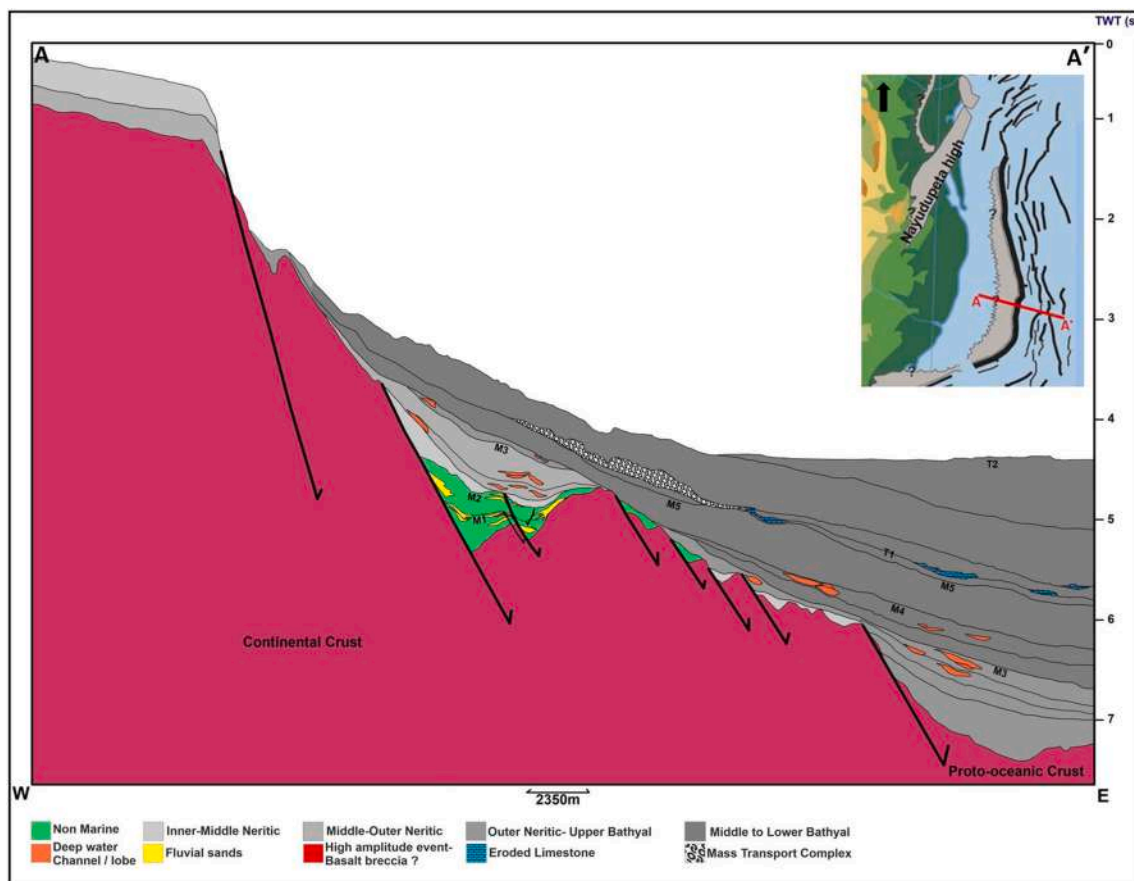


**Fig. 2.** Seismo-geologic cross-section across the Palar offshore pull-apart basin defining the tectono-stratigraphic markers and their thicknesses. The approximate location of the cross-section is shown in Fig. 1 as AA' line. M1, M2, M3, M4 and M5 are the first and the second order sequence boundaries/unconformity surfaces of Mesozoic, while the T1 and T2 are the sequence boundaries/unconformity surfaces of Tertiary (modified from Dasgupta, 2018a; Misra and Dasgupta, 2018a). Detail in Supplementary Fig. 1.

erosion with very less deposition of Late Cretaceous and Early Tertiary sequence, comprising of claystone with thin bands of siltstone deposited under marine environment. The equivalent unit deposited in Pennar basin during late post-rift drift phase is known as Raghavpuram Shale followed by Raghavpuram Sandstone in Late Cretaceous and Early Tertiary Periods, respectively.

Thus the Tertiary section in onland and shallow water Palar – Pennar basin is relatively very thin. Throughout Early to Mid-Eocene, a high-stand environment prevailed along the shelf to the upper slope part in major part of the east coast basins where carbonates deposited (Rangaraju et al., 1993; Bastia and Radhakrishna, 2012). In the deep-water Palar basin, the Early to Mid-Eocene period consists of limestone, which got eroded from the shelf to upper slope part (Bastia and Radhakrishna, 2012). Repository presents other geologic and tectonic details of the Palar basin.

### 3. Techniques used

A flow chart (Supplementary Table 3) presents the approaches taken in this work.

#### 3.1. Onland drainage analysis

We study remote sensing data to understand the tectonic imprints/lineament pattern and structural control over the drainage network. Integrated morphometric techniques and geometric data analysis are based on the 30 m CARTOSAT I DEM (2015).

#### 3.1.1. DEM Approach

DEM data specifications are provided in the Appendix. Five distinct watershed areas and drainage orientations have been delineated from the extracted DEM data. Morphometric attributes viz., relief, slope and aspect map are generated from each watershed. Two aspects of morpho-tectonic analyses have been adopted: in linear and spatial scale dimension. The D8 algorithm in the ArcGIS software has been followed to identify the flow directions on the topographic surface regarding streamline tracing from each pixel to its eight neighbouring pixels. Based on steepest descent, the algorithm is framed considering the directions from each pixel to its eight-neighbouring pixels. This algorithm is necessary to track individual channels, river networks and basin boundaries. This is based on two assumptions: (i) the use of discrete flow angles, and (ii) each pixel has a single flow direction (based on Arc GIS 10.3).

Google Earth Pro has been used to compare the extracted drainage lines. The watersheds have been delineated based on flow accumulation in Arc GIS 10.3. The incorporated relief characteristics, drainage parameters, linear aspects as long profiles, and morphometric techniques in terms of morpho-tectonic indicators signify the tectonic signatures. Indices of active tectonics has been estimated from the five watersheds, which provide reliable semi-quantitative assessments of the relative degree of tectonic activeness (Bull and McFadden, 1977; Silva et al., 2003; Mahmood and Gloaguen, 2012; Elias, 2015; Prakash et al., 2017; Elias et al., 2019).

We calculated basin shape index (Bs), circularity ratio (Rc), Hypsometric integral (HI), Elongation ratio (Re), Transverse topographic symmetry (T), and Form factor (Rf). The computed parameters are

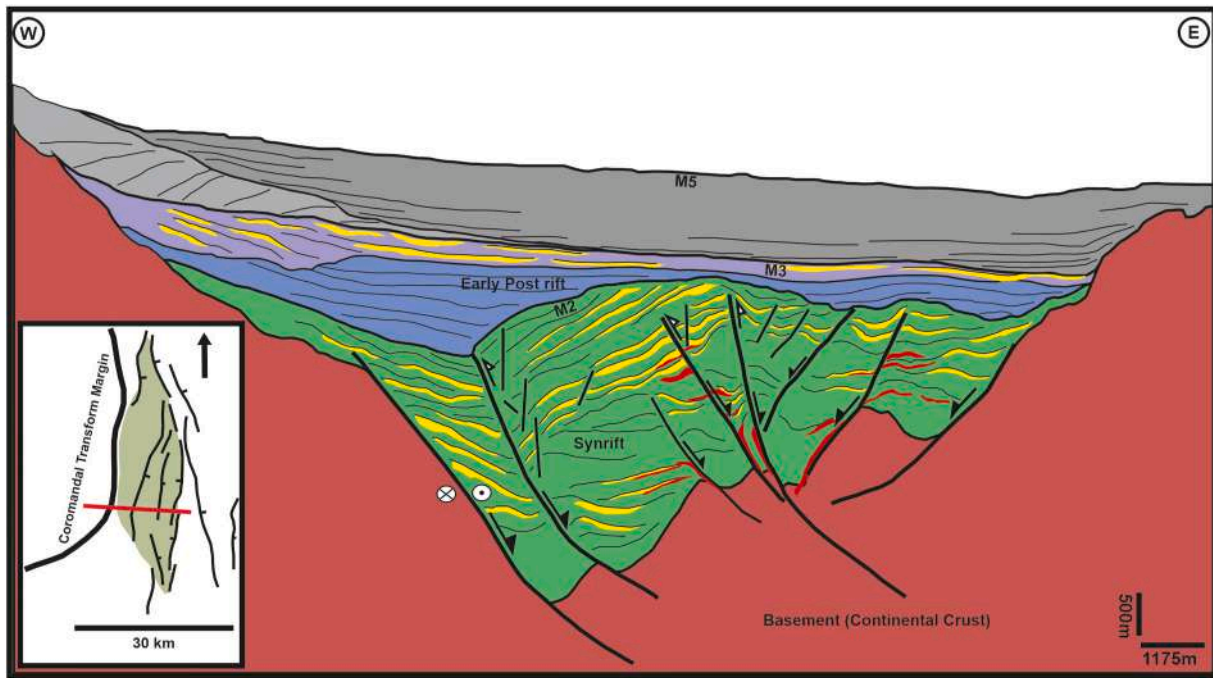


Fig. 3. Seismo-geologic cross-section across the Palar offshore pull-apart basin defining the first and the second order sequence boundaries/unconformity surfaces of Mesozoic with the corresponding stratal terminations (onlaps, downlaps and truncations; modified from Dasgupta, 2018a). Refer to Supplementary Figs. 1 and 2 for details.

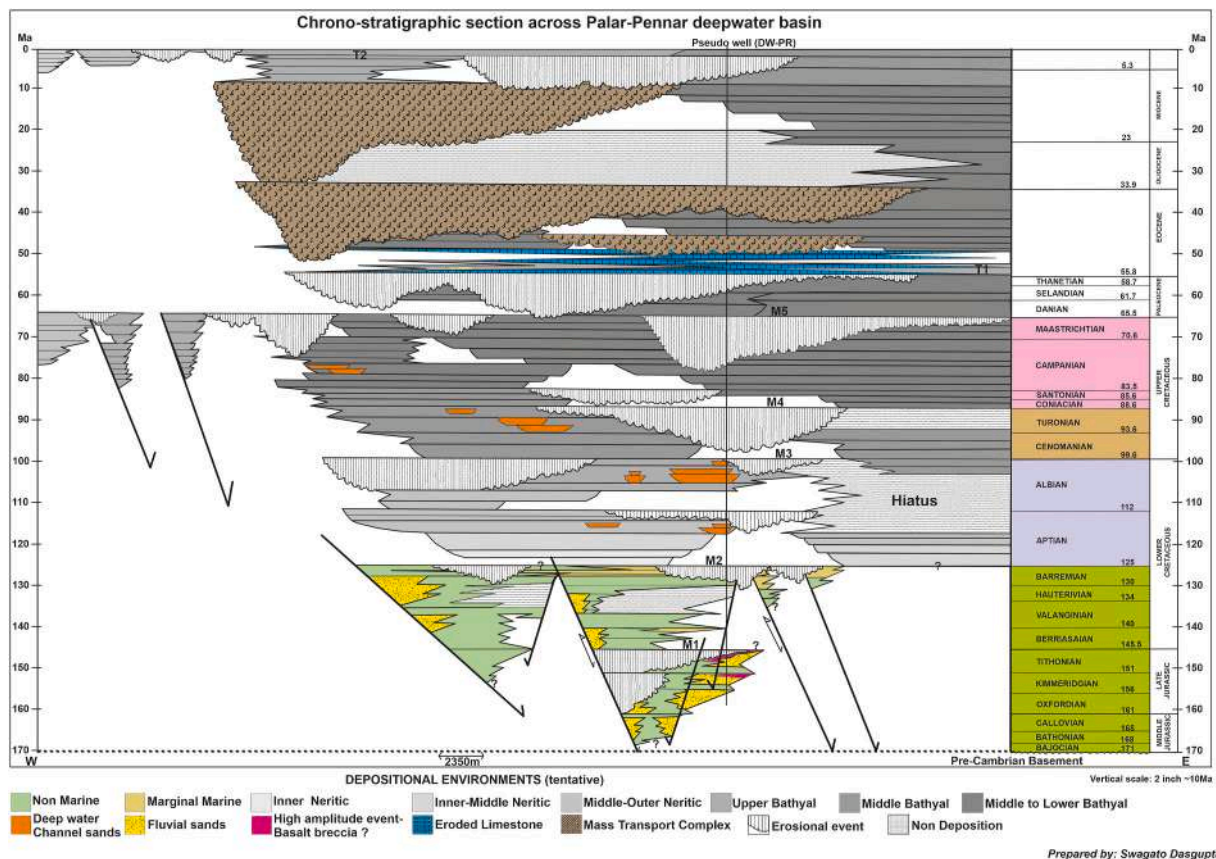


Fig. 4. Chronostratigraphic section along the line AA' in Fig. 1A across the Palar deep water basin illustrating the depositional pattern of different stratigraphic units with respect to tectonic changes. Note the ages are based on regional correlation and understandings from published literatures (Rangaraju et al., 1993; Gaina et al., 2007; Veevers, 2009; Lal et al., 2009; Bastia et al., 2010; Bastia and Radhakrishna, 2012; Nemčok et al., 2013a).

grouped into class-1 (high), class-2 (Moderate), and class-3 (low) as per Mahmood and Gloaguen (2012); the computed classes of each index are combined to yield the index of active tectonics (IAT). The calculated IAT is classed into three group viz. low, moderate and high activity. Computation of all aligned analysis has been adopted from Arc GIS 10.3 and Surfer 11 platform (detail in Table 1).

### 3.2. Stratigraphic architecture - offshore

Seismic stratigraphic analysis is a technique for stratigraphic interpretation from seismic reflectors (Vail et al., 1977). Such study associated with sequence stratigraphic analysis helps to identify petroleum system elements viz., reservoir facies, seal, and source pods (Vail, 1987; Catuneanu, 2006). Major unconformities/discontinuity surfaces can be identified considering the stratal terminations/seismic reflector relationship within a sequence to the corresponding sequence boundaries (Vail et al., 1977; Vail, 1987; Posamentier and Walker R, 2006; Misra and Mukherjee, 2018; Asl et al., 2019; Faghih et al., 2019). Seismic sequence stratigraphic study in deepwater settings (continental slope area) is more complex than the shallow water shelf part (Posamentier and Walker R, 2006; Catuneanu et al., 2009). Thus, identification of system tract in deep water settings is far more difficult and sometimes impossible to achieve, due to: (i) facies change, (ii) impact of gravity flows, (iii) change in sediment supply and dispersal pattern, and (iv) local accommodation changes due to variation of underlying topography.

#### 3.2.1. Works done

As an exercise in sequence stratigraphy (Repository Section 3; Figs. 2 and 3), about seven major unconformity surfaces were identified based on stratal terminations (onlap, downlap, erosional truncations). Mesozoic succession of around 1–2s TWT thickness composed of layer parallel relatively continuous reflectors, controlled by underlying topography, with occasional high amplitude packages (Fig. 2; Misra and Dasgupta, 2018a, Dasgupta, 2018a, b). The Tertiary sequence forms a wedge shape with maximum thickness of around 2s TWT in the deeper part towards east (Fig. 2; Misra and Dasgupta, 2018a; Dasgupta, 2018a, b). The whole system consists of high amplitude continuous reflectors except for some non-amplitude chaotic events indicating mass transport complex (MTC).

A chronostratigraphic section (Repository Section 4; Fig. 4) has been prepared from the sequence stratigraphic framework understanding along dip section across the transform margin setting. The onlap/downlap limits were critically delineated within each sequence by flattening the reflectors/events with respect to geological time scale. This helped in defining certain features like extent of erosion and non-deposition that were hitherto not understandable in the original seismic data. Considering erosional truncations at major sequence boundaries, erosional events at respective unconformity surfaces were demarcated. The section was then used to visualize different depositional events with respect to basin scale uplift and subsidence across the transform margin. The stratigraphic sequences are sub-divided into syn-rift and post-rift intervals as identified and conceptualized from the seismic stratigraphic study and constructed chronostratigraphic section. The post-rift unit is further sub-divided into Mesozoic and Tertiary post-rift intervals. As discussed in the introduction, Permo-Triassic pre-rift sediments occur in the onland Palar–Pennar basin. The pre-rift sequence likely to be present in some of the grabens in the offshore part; however they are poorly imaged in seismic data and are speculative, hence not taken up in the analysis.

#### 3.2.2. Syn-rift sedimentary sequence

In a syn-rift depositional setting, a fluvio-lacustrine environment in the initial to mid rift phase is expected, which successively changes to shallow marine shoreface to deltaic deposition towards the late rift phase (Ravnås and Steel, 1998; Bastia and Radhakrishna, 2012). In a typical strike-slip transform margin, the rifted segments are governed by

transtensional to transpressional movements. The transtensional motion generates a pull-apart type of rifted basin. These basins are normally characterized by rapid lateral facies change with respect to rapid subsidence (Miall, 1997).

In deepwater Palar basin, the syn-rift architecture is governed by a set of rotated fault blocks having varied extent of subsidence (Fig. 3). The syn-rift sequence is equivalent to Sriperumbudur Formation of the onland part (Rangaraju et al., 1993). The early syn-rift sediments are probably part of prograding alluvial fans from steeper footwall scarp. There can be also some occasional shales having organic rich materials (Ravnås and Steel, 1998). Thicker shales deposit plausibly in the basin centre in a lacustrine environment. Axial type braided systems are expected to be present along the low relief areas in the hangingwall slope. The axial channel facies may switch laterally depending upon the nature of subsidence and the extent of prograding transverse alluvial fan complex (Ravnås and Steel, 1998).

Two major sub-horizontal unconformity surfaces are identified in the syn-rift sequence (Figs. 3 and 4). The first one (M1) is between early and mid – late syn-rift, likely to be at the junction of Late Jurassic to Early Cretaceous. The age correlation, though not accurate, is based on the regional understanding of the Palar – Pennar basin (Vairavan, 1993; Basavaraju et al., 2016). This erosional unconformity delineates a major change in tectonic regime from early syn-rift to mid-to late syn-rift phase. The transition from granitic (granite gneiss) basement to early syn-rift (and/or pre-rift in some grabens) deposits are indistinct in seismic (Dasgupta, 2018a; Misra and Dasgupta, 2018a). Few volcanic intrusive bodies or eroded basaltic breccias could be present close to the faults as interpreted from the high amplitude reflectors. These volcanic bodies could be related to either (i) volcanic sill intrusion in the up-dip part of rotated fault block, or (ii) brecciated basalt, which intruded along the faults that later got eroded and subsequently deposited in vicinity to the fault zone. This could be a result of fast stretching during India-Antarctica separation (Nemčok et al., 2013a, b; Nemčok et al., 2016).

The mid to late syn-rift stage is governed by increase in subsidence rate of the hangingwall portion along rift fault. A dominant lacustrine environment is likely to prevail all along the basin (Ravnås and Steel, 1998). The deposits are primarily finer clastic i.e. organic-rich shale, occasional fine grained sands and silts (Ravnås and Steel, 1998). Syn-sedimentary growth in mid to late syn-rift section has been observed in seismic section, indicating fault re-activation (Fig. 3). Towards the end of syn-rift phase, during Hauterivian-Barremian time (~130-125 Ma), the basin uplifted, and subsequently erosion happened. The same has been captured in the constructed chronostratigraphic section (Fig. 4). This is possibly as a result of Antarctica having slid past towards south along the strike-slip margin, thereby forming new oceanic crust between the India-Elan Bank and Antarctica (Krishna et al., 2009; Bastia et al., 2010).

The second unconformity surface (M2) marks the end of syn-rift period and onset of early post-rift deposition. The M2 unconformity is very distinct basin-wide, identified by erosional truncations below and onlapping events above the surface (Figs. 3 and 4). This end of syn-rift unconformity surface (M2) is very distinct in many deepwater seismic sections (Dasgupta 2018a, b; Misra and Dasgupta, 2018a, b) and can also be correlated with onland and shallow water sections (Vairavan, 1993). Towards the end of rifting phase intermittent shallow marine influx happened as the basin subsided.

#### 3.2.3. Post-rift depositional system

The post-rift sequences have been divided into number of transgressive events in the continental slope part of the basin. These transgressive sequences have been interpreted from the seismic section based upon the onlaps and stratal terminations (Figs. 2 and 3; Dasgupta, 2018a, b; Misra and Dasgupta, 2018a, b). They are easily identifiable in chronostratigraphic section (Fig. 4). Note that the pull-apart basin is in eastern side of the Coromondal transform margin of Palar basin. Hence it

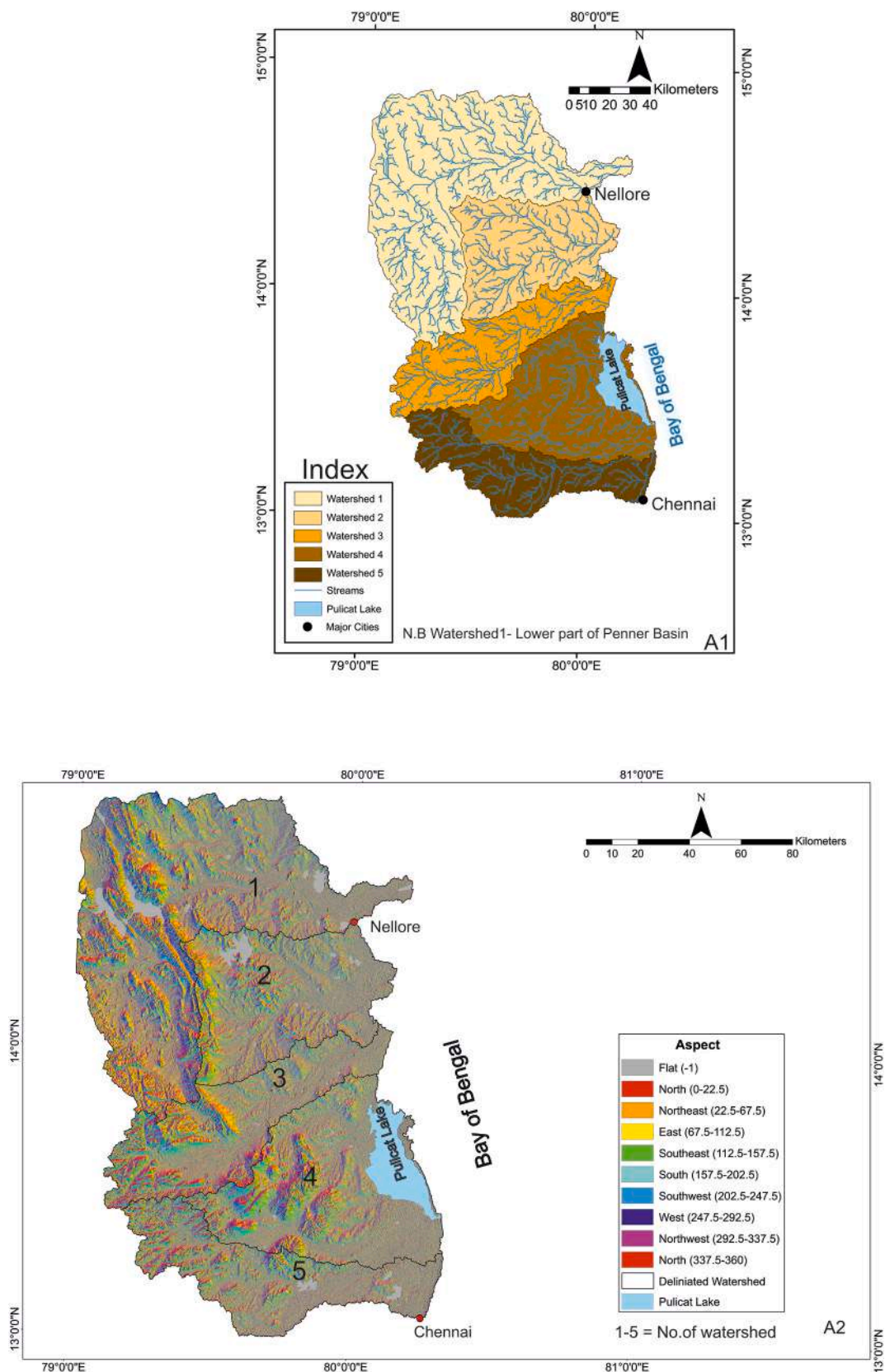


Fig. 5. (A1) Delineated 5 watershed of the study area where watershed 1 is the lower of part of Pennar river; extracted from DEM in Arc GIS (10.3) plat form. (A2) Aspects of slope direction map of the entire 5 watersheds where directions are represented in different colours on hill shade; extracted from DEM. (For interpretation of the references to colour in this figure legend, the reader is referred to the Web version of this article.)

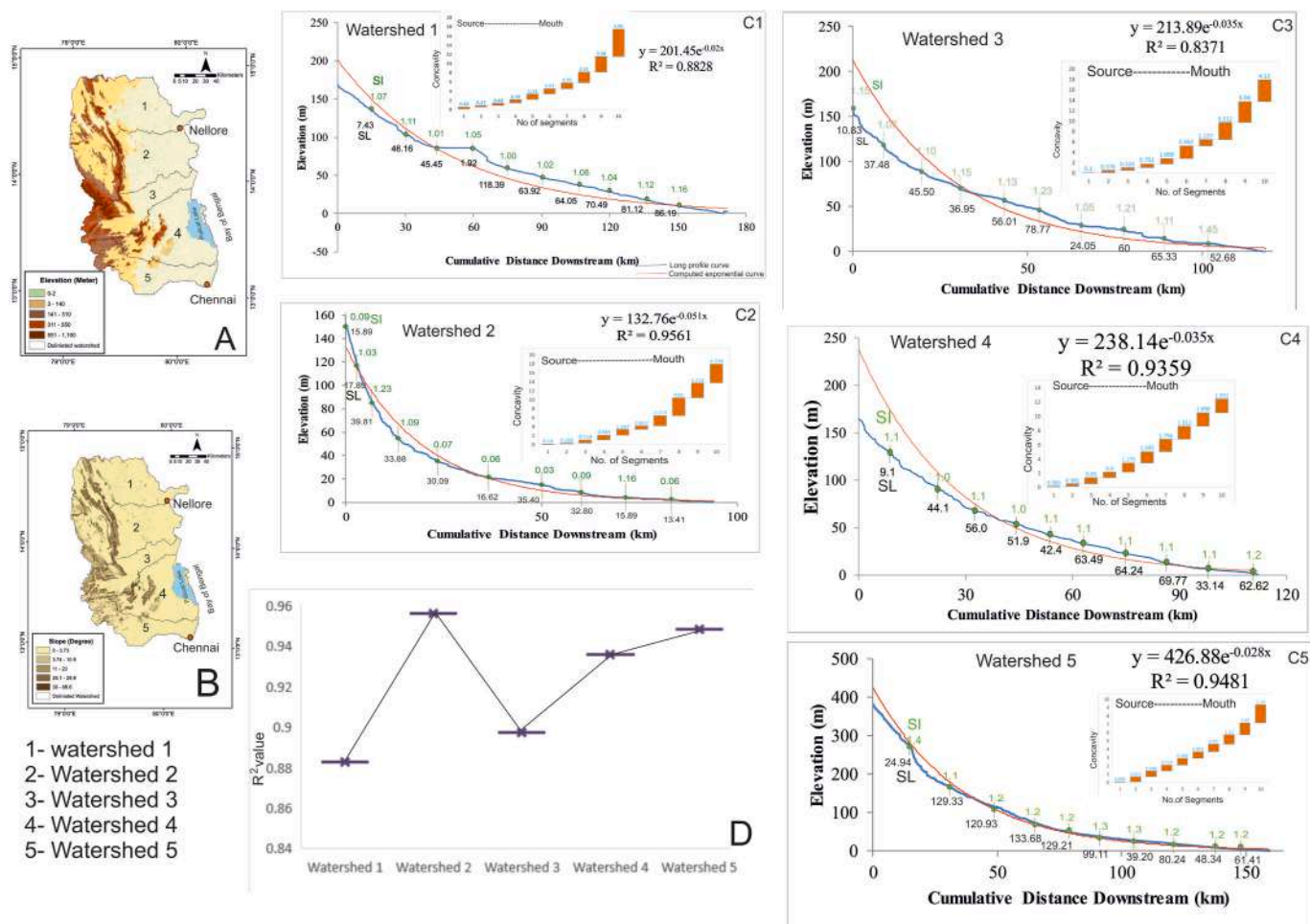


Fig. 6. (A & B) Elevation and slope(in degree) map represent elevation variation from ~1100 to 2 m, slope from 36.6 to 3.37°. Higher ranges of relief and slope are extended along the NNE-SSW range of Precambrian Cuddapah highlands. (C1 – C5) Exponential curve fit along each river long profile with distinct representation of SL and SI of 10 elevation segments. Calculated values of concavity define the erodibility of the channels at different segments. (D) Graphical layout of R<sup>2</sup> values of computed exponential curves. Watershed 2 and 5 trend towards the higher values than others. They intensify the highly positive trend lines.

is in mid to lower continental slope area where actual marine regression would not happen. Impact of the regressive phase taking place in shelf and upper slope parts will be expected in the lower slope in terms of coarser clastic fairways (Catuneanu, 2006; Catuneanu et al., 2009). About four to five unconformity surfaces related to key tectonic events have been identified based on stratigraphic terminations. These surfaces are M3, M4, M5, T1 and T2. Accordingly, the post-rift events are divided into respective tectono-sequences i.e. M2-M3, M3-M4, and M4-M5 in Cretaceous and M5-T1, T1 to recent (T2) in Tertiary (Fig. 4).

**3.2.3.1. Mesozoic post-rift interval.** The Early post rift sequence (M2-M3) of ~Albian-Aptian age is controlled by marine transgressive events onlapping onto uplifted synrift and basement fault blocks and basin margin escarpment surface (Figs. 2–4). Above this onlapping sequence there exists distinct down-lapping high amplitude units observed in seismic data, having geomorphic characters of lobes and fan like geometry (Figs. 23.2 and 23.3 in Dasgupta, 2018a). These are interpreted as slope fan bodies deposited possibly during post-rift Early Cretaceous time - Mid to Late Albian (Figs. 3 and 4; Ravnås and Steel, 1998; Zachariah et al., 2009; Nemčok et al., 2016). This indicates a regressive environment prevailed in the shelf to upper slope area. Sub-aqueous eroded sediments of shelf and upper slope area got deposited in the mid to lower slope part. This event could be a direct consequence of Elan bank sliding past the eastern margin of the Palar-Pennar basin possibly alongside the transform margin immediately after its separation from

the Indian east coast. The M2 – M3 sequence thins out thereby developing condensed section/non-deposition over the uplifted fault block and on the escarpment side (Figs. 2 and 4). This was followed by a subsequent tilting towards E to SE, as observed from sequential onlapping events (Figs. 2–4). It implies that basin subsidence in the eastern part could be a consequence of the Elan Bank’s separation (Bastia et al., 2010). The M3 – M4 and the M4 – M5 sequences, equivalent to Late Cretaceous, are of reduced thickness comprising of onlapping sequence in a transgressive system. In seismic section these intervals consists of low amplitude parallel to onlapping reflectors indicative of finer clastics (Nemčok et al., 2016; Dasgupta, 2018a). The Madagascar separation towards the end of Turonian (88–84 Ma; Storey et al., 1995; Reeves, 2013; Chand and Subrahmanyam, 2013) isostatically uplifted the southwestern margin of the Indian peninsula. As a consequence, the onland and offshore Cauvery basin consists of thick Late Cretaceous coarser clastics (Rangaraju et al., 1993; Chaudhuri et al., 2009; Nagendra and Reddy, 2017; Dasgupta, 2019). However, this event had little impact in the offshore Palar basin. Even in the onland/shallow water part of Palar basin, the Late Cretaceous thickness is very less (Vairavan, 1993; Vaidyanadhan and Ramakrishnan, 2008). The Cretaceous top unconformity surface (M5) is very distinct in deepwater seismic sections (Nemčok et al., 2016; Misra and Dasgupta, 2018a; Dasgupta, 2018b) and is marked by erosional truncations at the bottom and onlaps on top of it. This is well evident from the constructed chronostratigraphic section (Fig. 4).

**3.2.3.2. Tertiary sequences.** The whole Tertiary system is divided grossly into two units. The first one is the Early Tertiary sequence (M5–T1). The second sequence, T1 – T2, is composed of largely Eocene – Miocene to Recent deposits. During Paleocene, the basins along the east coast margin of India encountered high sedimentation and subsidence rates (Dasgupta, 2018b). Uplift of western part of the peninsular India due to Deccan volcanism probably tilted the Indian plate due SE (Kailasam, 1979; Subbarao et al., 1994; Subramanian, 1987; Widdowson, 1997; Collier et al., 2008; Veevers, 2012; Misra et al., 2014). This tilting could be the reason of high sedimentation and subsidence rates in the east coast basins during Tertiary. The sediment distribution of M5 –T1 sequence, in the Palar offshore deepwater basin along the transform margin, is quite varied i.e. in many areas it is largely sediment starved whereas in some parts there is rapid sedimentations and erosion as observed from seismic data (Nemčok et al., 2016; Dasgupta, 2018a, b; Misra and Dasgupta, 2018a). This can be understood from the constructed chronostratigraphic section (Fig. 4).

The later part of T1 –T2 sequence is dominated by backstepping onlapping wedge-out sequence (Figs. 2 and 4). There are large-scale erosional mass transport complexes (Figs. 2 and 4) in the Late Tertiary sequence (T1 to T2), probably due to erosion at shelf edge-upper slope area along the steep Coromondal transform margin. This might be a consequence of hydraulic instability during rapid sea level rise (Condie, 1993; Nagendra and Reddy, 2017; Anomneze et al., 2020).

#### 4. Results and discussions

The study area (Fig. 1A–C) of the Palar–Pennar basin, both the offshore and the terrestrial parts, is tectonically significant in its spatial entity. The pre-existing basement fractures and lineaments play a major role in the basin tectonics, drainage and sediment deposition pattern implying the role of structural inheritance in the basin. The onland terrestrial part and the offshore area of the basin have been discussed in two separate segments as provided below. There is no direct linkage between the geomorphic/morpho-tectonic analyses of the onland terrestrial part and the offshore depositional systems. However, the reason to study the onland part is to understand the tectonic imprints – as the tectonic events would have affected entire basin area to some extent.

##### 4.1. Onland Palar – Pennar basin

The terrestrial part of the upper Palar–Pennar basin is composed of five distinct watersheds (Figs. 1C and 5A1) drained by Pennar river and other secondary rivers. Watershed 1 is the lower part of Pennar river and other streams originate from the western Cuddapah highlands, flowing across the terrain following the lineaments and fractures and ends into the Bay of Bengal. These lineaments are the major controlling factors in configuring the drainage orientation, direction and density. The prepared aspect slope map (Fig. 5A2) indicates the different direction of slope that connects the channels, forming different drainage patterns. Four kinds of linear drainage analyses have been performed as Strahler stream order, drainage pattern, drainage density ( $\text{km}/\text{km}^2$ ), and long profile.

The drainage density (Dd) maps of the individual basins determine the concentration of drainage lines in  $\text{km}/\text{km}^2$ . Morphologically, more drainage lines join the main channel over the middle part of the watersheds; induced by tectonic anomalies such as lineaments and minor fractures, which govern the flow pattern following the local gradient (Supplementary Fig. 3A–F). The maximum values of drainage densities are found from watersheds 2 and 5 (3.71 and 4.11, respectively) as they cross both across and along the lineaments (detail in Repository Section 5).

Geomorphologic parameters have been successfully used as indicators of tectonics (Prakash et al., 2017; Wołosiewicz, 2018). The normalized long profile analysis with logarithmic curve fit and

calculated  $R^2$  values proves that the region is neo - tectonically active (Bhatt, 2020; Biswas and Paul, 2020; Biswas et al., 2021). Several NE, ~ E and NW lineaments occur in the study area (Fig. 1C, rose diagram in Fig. 1C1). The elevation and the slope maps (Fig. 6A and B) give overall ideas of relief and amount of slope in different geomorphic units e.g., ridges, scarps, valleys, low coastal plain and littoral coastal section. The classified five classes of slope of the study area vary from zero near the shoreline to  $86.6^\circ$  in the elevated elongated section of Proterozoic Cuddapah range. Lower slope angles denote lower ruggedness and high erodibility that is accompanied by dissection mechanism of rivers. The calculated  $R^2$  values in the exponential curve of all the master streams of the watersheds vary from 0.837 to 0.956 (Fig. 6C1–C5).  $R^2$  shows a good fit of the regression model amongst the parameters.  $R^2$  values explain the variance of the relationship with the best fit (Lee and Tsai, 2009) (Fig. 6D). It significantly indicates that all the riverine sections are tectonically active.

Amongst them, watershed areas 2 and 5 are strongly determined by a number of tectonic anomalies that have experienced deformation during different tectonic episodes from Precambrian (Venkatakrishnan and Dotiwalla, 1987; Nagaraja Rao et al., 1987; Chetty and Bhaskar Rao, 2006; Mazumder and Eriksson, 2015), which in turn governed the later tectonic activities. The value of concavity up to 0.7 for each master stream denotes active tectonics, but alternative or stratified changes of values along the channel indicate slope differentiation, which is associated with tectonic episodes (details in Repository).

Amine et al. (2020) argued that channel diversion and alignment set a variety of line arrangements, termed as drainage pattern, which are closely associated with rock characteristics (vide Repository). In the onland studied area, the drainage pattern varies from lineament guided in the western upslope to dendritic in the downslope towards coast (Supplementary Fig. 4A and B). The tree-like arrangements and random orientation of channels form dendritic drainage patterns indicate a homogeneous basement. This pattern retains as an invariant structure that is well identified in the lower part of watersheds 1, 2, entire 3 and part of 5. Here, the channels of watershed 1, 2, entire 3, and part of 5 acts as a respondent to the tectonic perturbations (Castellort et al., 2012). In the upper catchment, towards west, a part of watershed 4 formed rectangular drainage pattern where secondary drainage lines have joined at a right angle following the basement lineaments (Supplementary Fig. 4B). The logarithmic profiles with best-fit curve re-examine the tectonics, as earlier, where the  $R^2$  values are positive with ranges between 0.808 and 0.977 (Supplementary Fig. 4C). The assemblage of five normalized watersheds clearly displays the concave pattern of each channel with break of slope due to faults and fractures (Supplementary Fig. 4C).

The topographic distance with thalweg differences are the assemblage effect of different vertical erosion rate, rock resistance, and climatic changes over time (Hack, 1957). Thus, channels have curved the spurs and ridges sequentially where the stream length gradient and sinuosity values have changed alternatively. These features act as an indicator of lithologic impact on longitudinal profiles and examine whether the rivers have attained their equilibrium or not.

Keller and Pinter (2002) referred to the stream length-gradient (SL) index to assess the relative tectonic activity of an area. The SL values of the five watersheds vary from 1.92 to 133.68 (Fig. 6C1 –C5). Comparison and analysis of random alteration of SL values along the long profile of each watershed distinctly relate to the tectonic activities. In general, the higher values along the channel connote to the younger and recent tectonic activities and inconsistent low values are associated with pre-existing fractures where the channels flow along or across them (Keller and Pinter, 2002).

The study reveals anomalies in the sinuosity index (SI), i.e. ratio of channel length to valley width, and concavity from source to mouth of the main channels within the respective watersheds. SI indicates the channel incision or down cutting in either straight or sinuous manner. Straight and sinuous flow pattern of channel regulate the channel flow through any weak zones such as faults or fracture planes. Such pattern

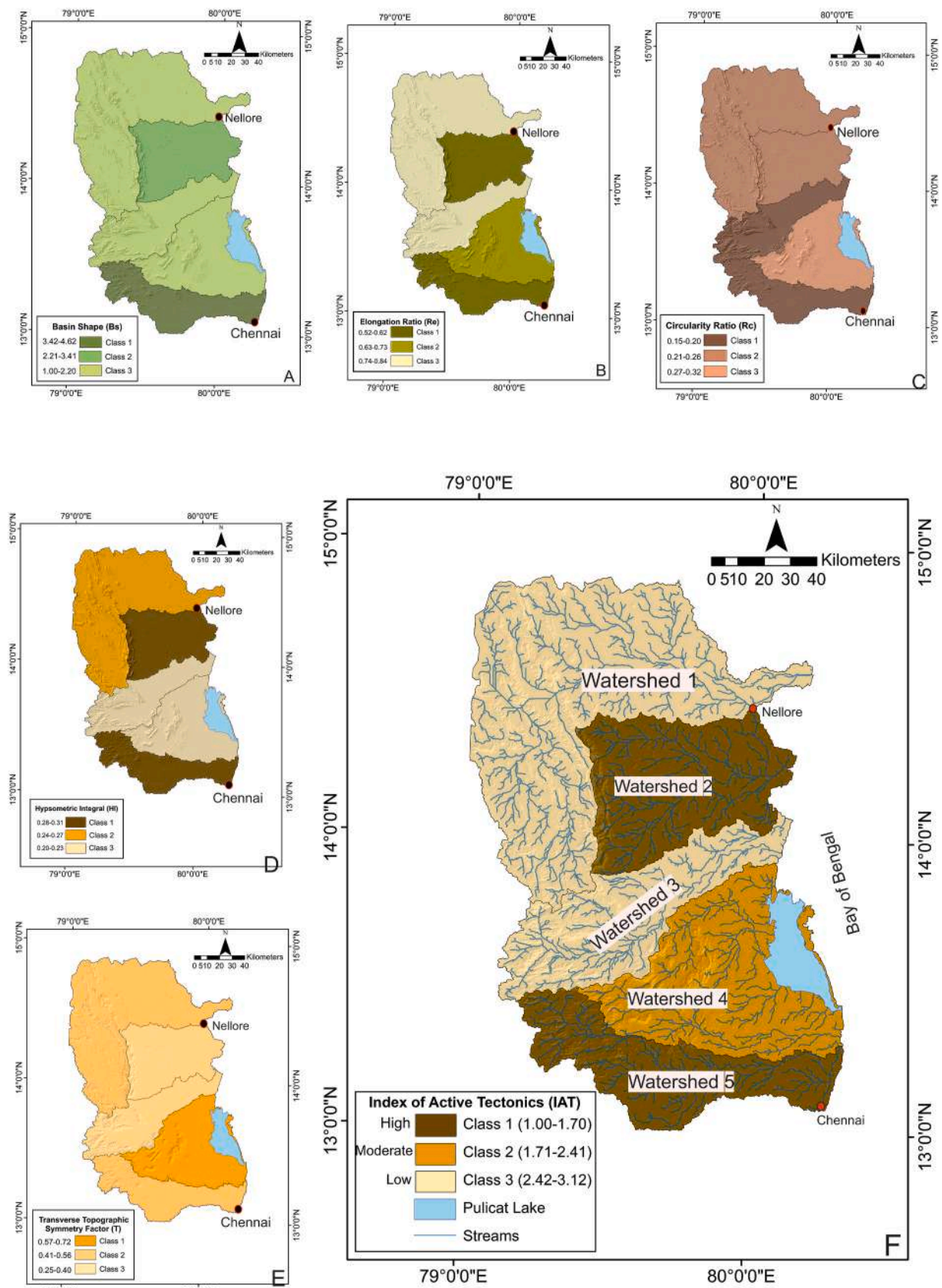


Fig. 7. (A-E) Spatial layout of the selected basin scale parameters as basin shape index, elongation ratio, circularity ratio, hypsometric integral, and transverse topographic symmetry factor for the analysis of Index of Active Tectonics (IAT) with respect to 5 watersheds. (F) Index of Active Tectonics map considering 5 watersheds with three defined classes as class 1-high, class 2-moderate and class 3- low.

**Table 2**

**A:** Calculated values of different Basin scale parameters of 5 considered watersheds with their classification. **2B:** Ranking of calculated values for the assessment of indicator of active tectonics (IAT) and classification of tectonic activeness amongst the watersheds.

Watersheds	Basin shape Index (Bs)	Elongation Ratio(Re)	Circularity Ratio(Rc)	Hypsometric Integral(HI)	Transverse Topographic Symmetry(T)	Form Factor (Rf)
Watershed 1	1.04	0.76	0.215	0.24	0.41	0.46
Watershed 2	3.25	0.55	0.258	0.28	0.28	0.24
Watershed 3	1.38	0.74	0.185	0.22	0.36	0.43
Watershed 4	1.6	0.73	0.29	0.23	0.68	0.42
Watershed 5	3.53	0.52	0.15	0.3	0.54	0.21

Classification						
Class 1	3.42-4.62	0.52-0.62	0.15-0.20	0.28-0.31	0.57-0.72	0.21-0.31
Class 2	2.21-3.41	0.63-0.73	0.21-0.26	0.24-0.27	0.41-0.56	0.32-0.42
Class 3	1.00-2.21	0.74-0.84	0.27-0.32	0.20-0.23	0.25-0.40	0.43-0.53

**A**

Watersheds	Ranking for IAT calculation						IAT
	Basin shape Index (Bs)	Elongation Ratio (Re)	Circularity Ratio (Rc)	Hypsometric Integral (HI)	Transverse Topographic Symmetry (T)	Form Factor (Rf)	
Watershed 1	3	3	2	2	2	3	2.5
Watershed 2	2	1	2	1	3	1	1.67
Watershed 3	3	3	1	3	3	3	2.67
Watershed 4	3	2	3	3	1	2	2.33
Watershed 5	1	1	1	1	2	1	1.17

**B**

Classes	Value	Tectonic activeness
Class 1	1.00-1.70	High
Class 2	1.71-2.41	Moderate
Class 3	2.42-3.12	Low

has minimum capacity of lateral erosion, rather it is involved in rigorous vertical cutting to form straight to sinuous pattern in an alteration mode from source to mouth (Repository Section 5). It is remarkably related to the concavity in response to gradient and erosion competency and related to power law function (Lee and Tsai, 2009). However, alteration of concavity values in watershed 1 and 2 along the channel determine the erosion competency and capacity. The alternating SI values viz., straight to sinuous to again straight denotes tectonic disturbances (Fig. 6C1-C5). Alternate elevation changes due to uplift enhance the vertical incision rate. It is associated with the extent of erosion regulating the concave or convex shape along the channel.

The other applied geomorphologic linear and special scale methods for analysing tectonic signatures are: Basin shape index (Bs), Elongation ratio (Re), Circularity ratio (Rc), Hypsometric integral (HI), Form factor (Rf) and Transverse Topographic Symmetry Factor (T) (Fig. 7; Table 1 for definition, Table 2A for calculated values).

Morphologically, in general the elongated river basins are near-parallel shaped to the topographic slope and become circular with time. Thus tectonically active basins, e.g. watersheds 2 and 5, are more elongate in shape, having higher basin shape index (Bs) value (Fig. 7A; Table 2A). The tectonic activeness of a basin reduces in circular-shaped basin temporally and continues evolving the topography in a systematic order of erosion/depositional sequence. It occurs when the river widens

but the transverse width reduces. In contrast, lack of slope-breaks and rapid uplift, restricts the down-cutting and thus widens the valley. Cuong and Zuchiewicz (2001) classified the elongated basins more accurately introducing three classifications as < 0.50 = tectonically active, 0.50–0.75 = less active, and >0.75 = inactive. Both classifications by Cuong and Zuchiewicz (2001), Pareta and Pareta (2011), have been applied. All the calculated elongation ratio (Re) values of the considered watersheds are in the range of: 0.5–0.75, which portrays that these watersheds are under relatively less active tectonics, exception can be watershed 1 with Re value 0.76 indicating tectonically stable area (Fig. 7B; Table 2A). The tectonic activeness is relatively higher in watersheds 2 and 5 (Table 2A). In comparison to elongation ratio, the circulatory ratio (Rc) also relates to tectonic activeness. Similar to watersheds 3 and 5, the Rc values are of 0.185 and 0.15, respectively (Fig. 7C; Table 2A; Pareta and Pareta, 2011).

The low values of HI (0.20–0.23) in watersheds 3 and 4 indicate old eroded landscape, which is in between mature and the old stage. The tectonically active area is designated by relatively higher values of HI as in watersheds 2 and 5 (0.28–0.31; Repository Section 5). Thus, in terms of HI index, watersheds 3 and 4 are in more mature stable tectonic stage than the erosive watersheds of 2 and 5 (Fig. 7D). Watershed 1 is moderately erosive (Fig. 7D). The computed HI values denote that the east-sloping steep ridges, in the western part of the study area, belongs

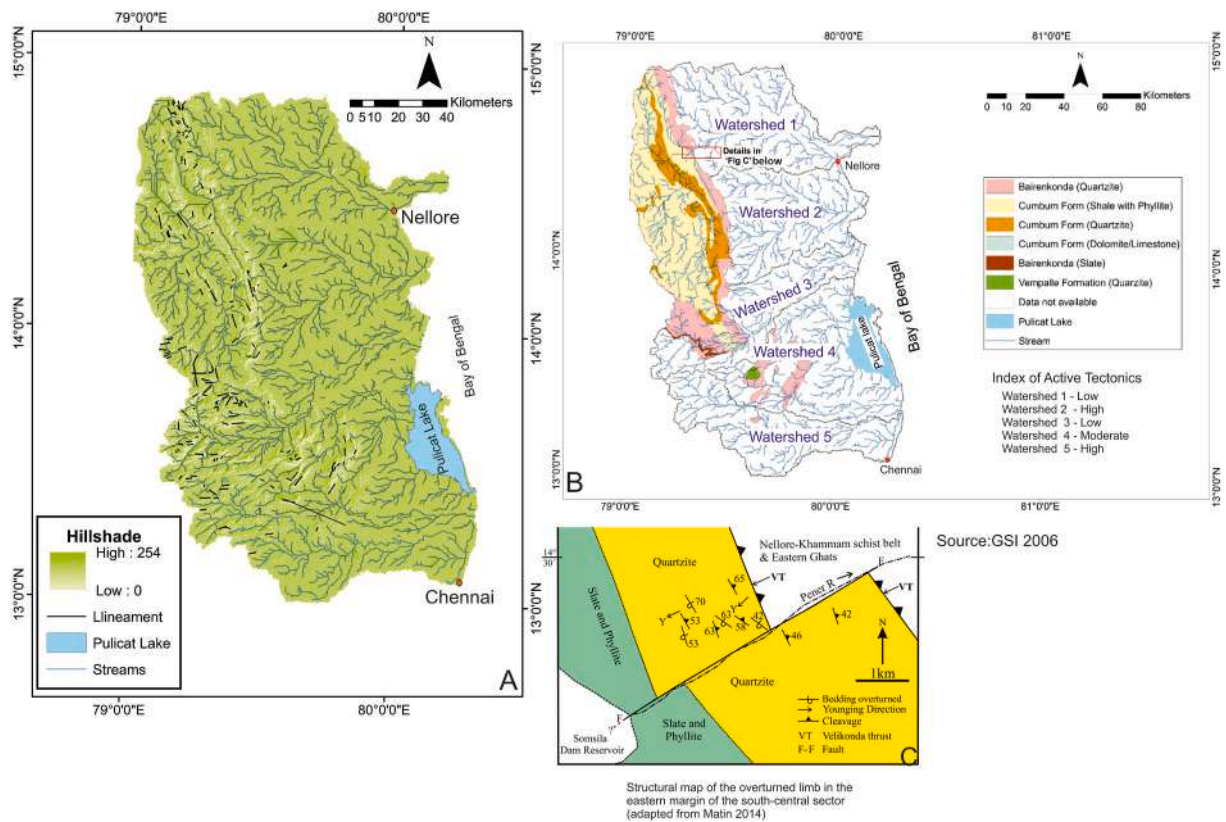


**Fig. 8.** (A) Extracted lineaments from DEM and hills shade (Arc G is 10.3) of the study area; aligned in different directions; drainage lines closely formed following the same direction. (B) Broad geological map of the study area embedded on drainage lines. Location of Fig. 8C marked in red. Source: GSI (2006). (C) Slip of shale/phyllite and quartzite beds due to SSW- NNE aligned fault line along the Penner channel. Structural map of the overturned limb in the eastern margin of the south-central sector (Matin, 2014). (For interpretation of the references to colour in this figure legend, the reader is referred to the Web version of this article.)

to the most young topography (watersheds 2 and 5), comprising of numerous discontinuities related to faults and lineaments. In watershed 5 ~NW trending major lineament is cut by ~NE trending small parallel lineaments. The arrangements of bi-directional lineaments induce higher erodibility and incision of the channels leading to higher HI values.

The transverse topographic symmetry factor (T) defines the ratio of: (a) distance between the midline of the drainage basin (watershed) and the active meander belt midline and (b) distance between the midline and the basin divide (Fig. 7E, Table 1). As per the formulated classes of transverse topographic symmetry factor, watershed 4 falls under class 1, watersheds 1 and 5 under class 2, while watersheds 2 and 3 under class 3 (Fig. 7E). Form factor has been calculated for all 5 watersheds for incorporating the indicator under IAT. The computed values from 0.21–0.31 under class 1 (watershed 2 and 5), from 0.32 to 0.42 as class 2 (watershed 4), and 0.43–0.53 belong to class 3 (watershed 1 and 3).

The calculated ‘T’ value is the reference of tilting of the basin. The lower values indicate the symmetry or the minimum tilt of the basin from the mid-line e.g., watersheds 2 and 3. The watersheds like 1, 4 and 5 render the asymmetric nature with moderate river oscillation and tectonic tilt terrain (Table 2A).

To provide a better configuration (details in Repository Section 5) and assessment of the tectonic status of the region (Ziyad, 2014), all the selective indicators are assembled for assigning the index of active tectonics (IAT) or the index of relative active tectonics (IRAT) (Mahmood and Gloaguen, 2012). This is obtained by the averaging out the different classes of geomorphic indices and then classifying them into three or four classes. Identically, there are 3 classes based on the results of IAT (Table 2B) where watersheds 2 and 5 denote high in tectonic activeness (1.00–1.70), 4 is moderate (1.71–2.41), and 1 and 3 are under low range (2.42–3.12) of tectonic activeness (Fig. 7F).

Most of the lineaments are parallel to the NW trending ridges of Cuddapah basin (Fig. 8A). The drainage lines of the upper catchment of watersheds 1, 3, 4 and 5 are specifically controlled by the aligned lineaments (Fig. 8A–C, Repository Section 5).

From the morpho-tectonic indicators and by observing Google Earth Pro images, five lakes and/or depressions were identified to be affected by tectonic changes. In the western part of the study area, along the NW trending ridges of Cuddapah basin dissected by ~NW lineaments, there are two ~NNW elongated, sigmoid shaped, tectonically depressed lakes sub-parallel to the extracted lineaments (Fig. 1B and C, 9A). The typical sigmoid shape indicates a transtensional tectonic activity (e.g. Nabavi et al., 2019), possibly occurring during Early Cretaceous. Thus the pre-existing Precambrian structural fabric and lineaments governs the topography of the lakes 1 and 2 (Fig. 9A–D).

The 3D display with Google Earth image and contour layout specifies that the lakes 1 and 2 (Fig. 9B–D) developed on a low elevated zone and expanded as a flat-water body where river lines merges with the lakes. There is another evidence of ~N elongated depressed lake like feature (no. 3, Fig. 9A), in the eastern margin at the coastal junction of watersheds 2 and 3 of the study area, that is not as prominent as lakes 1 and 2. In comparison to these three lakes, the Pulicat Lake, (located between Nellore and Chennai) is also elongated, and influenced by such tectonic movements. Major part of the watershed 4 drains into the Pulicat lake. It is morphologically defined as tombolo and highest length as 60 km in comparison to the other three having 19.48, 22.5 and 13.69 km lengths, respectively (Fig. 9E).

The selected fifth lake at the southern part of the onland Palar – Pennar basin, immediately N of Palar river, also coincides with the tectonic lineament of the area (Figs. 1B and 9F). It is an elongated rhomboidal lake extended in NNE direction and the length/width ratio is 1.5 (Fig. 9F). This lake is near the lower part of the Palar river basin,

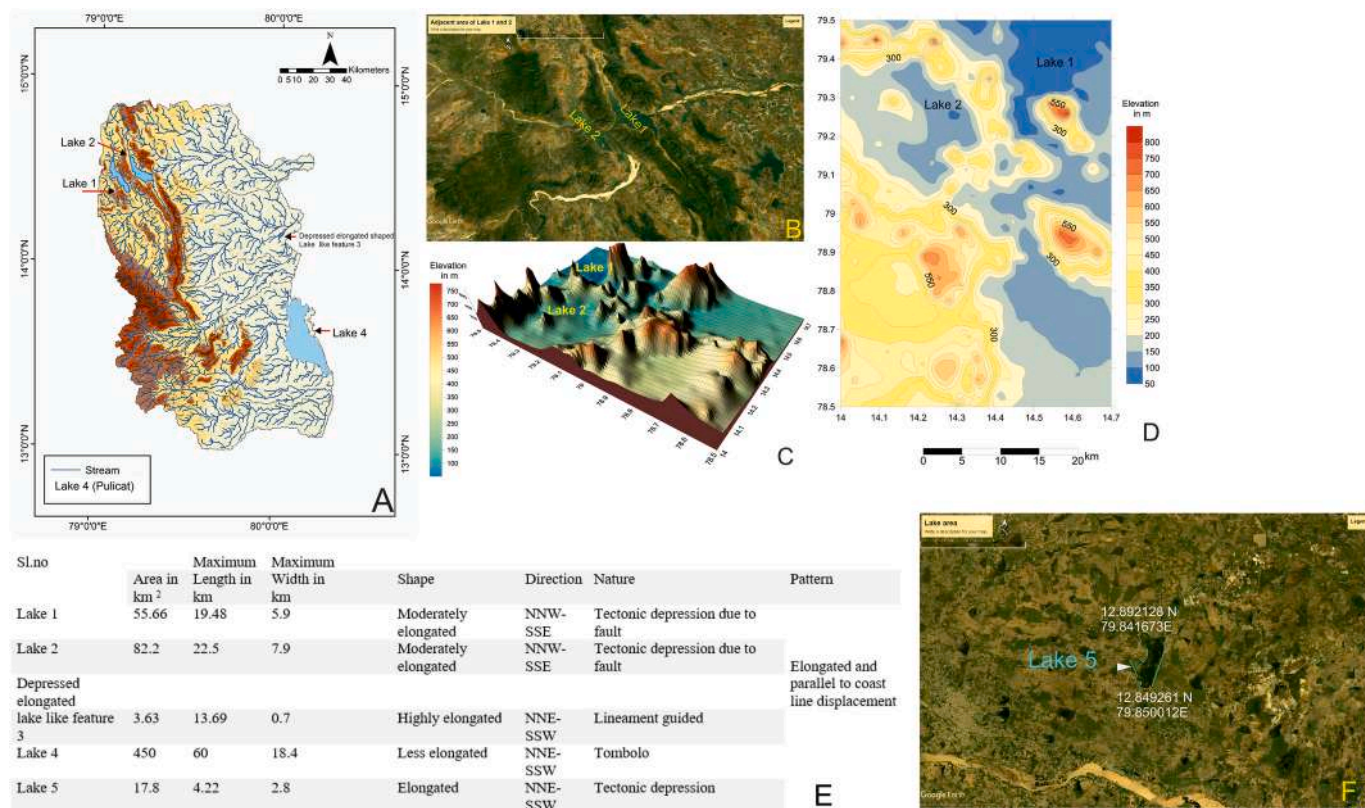


Fig. 9. (A) Identified elongate shaped lakes in NNW-SSE direction placed on relief and drainage layout map. (B) Location of Lake 1 and 2 on Google earth image. (C) 3D view of lakes 1 and 2 considering the adjacent terrain. (D) Spatial pattern of contours at an interval of 50 m projected on Lake 1 and 2. (E) Geometry of five lakes in terms of - area, maximum length, minimum length, direction, shape, nature and pattern. (F) Location of Lake 5 on Google earth image; situated northern side of Palar river towards downstream.

which significantly carries information on tectonics through morphometric analyses. Resmi et al. (2016, 2018, 2019) recognized the tectonically uplift-induced drainage system of the Palar river basin and also discussed the tectonic interference in the drainage morphometry. Therefore, for better understanding, the terrestrial tectonic control on channel geometry may be compared with the sea-bottom drainage orientation (to correlate the geometric results related to tectonic control) in offshore area of Palar basin along the Coromandal transform margin, which is quite similar to the Nellore-Chennai bay area, with the application of channel geometry. The marine bathymetric study (Susanth et al., 2021a) encompasses a number of parallel arrangements of streamlines oriented ~ NW following the coastal curvature. The geomorphic elements like foreword steep slope, two-step terraces, straight channel, axial incision, gorge like valley cutting, stoss and lee side's slopes (1.6–4.8), aspect ratio (ratio between sediment wave height and wave length), and asymmetry ratio acts as the indication of recent tectonics in the basin (Susanth et al., 2021a). Thus evidence of neo-tectonic activities and fracture guided drainage pattern are well recognized from the onland study area of Pennar river basin. The evidences are aligning to the offshore sea bottom geomorphic analysis of Palar basin along the transform margin (Susanth et al., 2021a, b).

#### 4.2. Offshore Palar – Pennar basin

A typical continent – ocean transform margin consists of few characteristic features: (i) a substantially steep and narrow thinned continental crust at the transition zone from continental to the oceanic crust, (ii) presence of a marginal ridge with raised pinnacle highs at the edge of the continental crust, and (iii) a high geothermal gradient with one or more thermal disturbances/pulses (Basile et al., 1993, 1998, 2012; Antobreh et al., 2009; Nemčok et al., 2016). The thermal perturbations

along with frictional heating along transform margin are also associated with hydrothermal fluid flows (Nemčok et al., 2016). The Coromondal transform margin in offshore Palar basin consist of such features (Nemčok et al., 2013a, 2016; Dasgupta, 2018a; Misra and Dasgupta, 2018a) with narrower shelf and continental slope and having contrasting bathymetry across the transform zone. This dextral strike-slip margin is a part of fast extension continental margin setting and is fairly comparable to the Côte D'Ivoire - Ghana transform margin, which is a part of the west African continental margin with an intermediate extension setting (Nemčok et al., 2013a, 2016). The Coromondal transform margin is associated with near orthogonal rift zones, i.e. K-G and Cauvery rifts, the two ends of a horse tail structure (Fig. 10 in Nemčok et al., 2016). The lateral extent of the syn-rift in the offshore Palar - Pennar pull-apart basin adjacent to the Coromondal transform margin is much narrower than that across the Cauvery deep water rift basin situated in the southern part of the horse tail of the transform margin (Dasgupta, 2018a; Misra and Dasgupta, 2018b; Dasgupta and Maitra, 2018). The thickness of syn-rift is more within the pull-apart basin towards western side of marginal ridge, while the syn-rift unit drastically dies out on the eastern side of the marginal ridge (Fig. 2, Nemčok et al., 2016). This is well understood from the constructed chronostratigraphic sections across the two basins (Figs. 4 and 10). The Cauvery offshore basin is a typical marine rift basin having a faster rate of extension, thereby having thicker synrift succession across all the sub-basins with a gradual to incremental sea level rise (Fig. 10, Rangaraju et al., 1993; Chaudhuri et al., 2009; Nemčok et al., 2013a, b; Dasgupta and Maitra, 2018; Maitra, 2018).

Across a transform margin, the difference in thickness between continent and alongside oceanic crust in association with variation in thermal regimes likely to have generated steep continental slopes along the transform margin (Basile et al., 1998). The stratigraphic response is

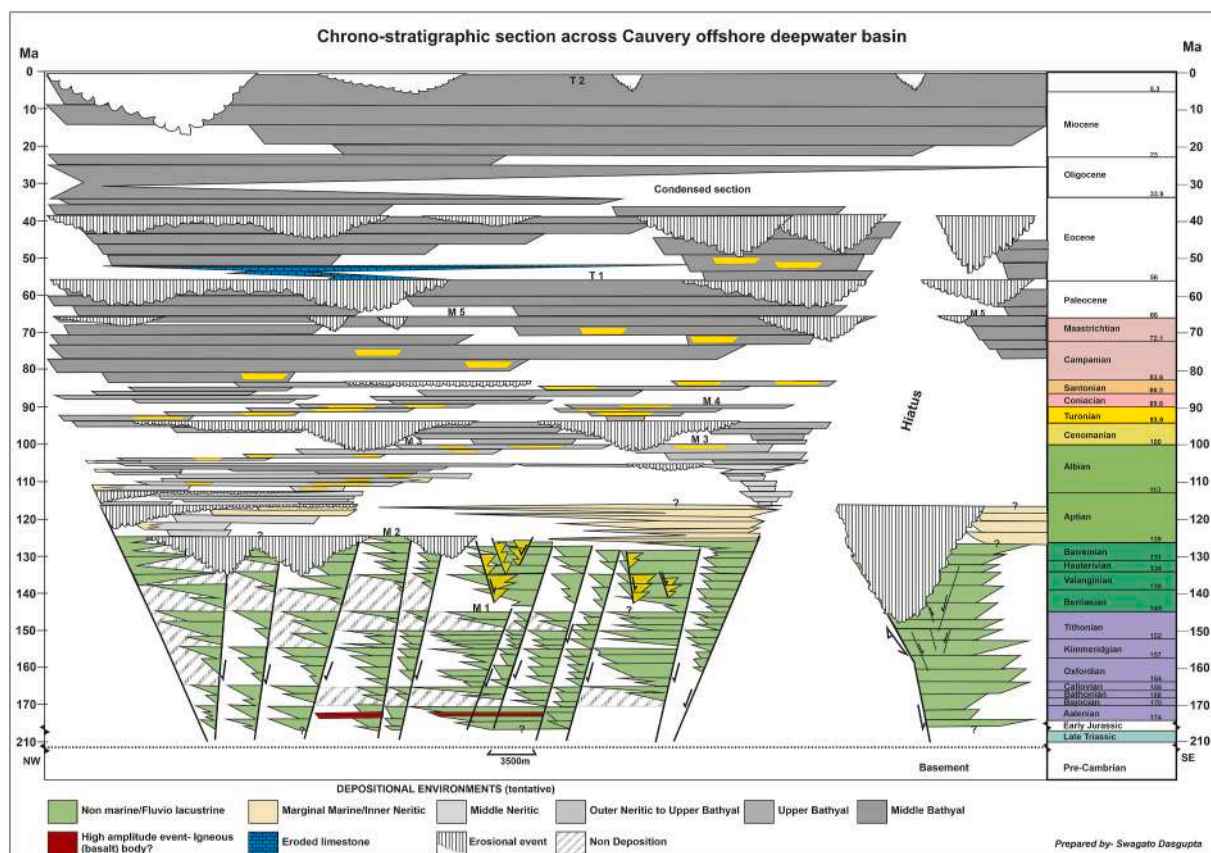


**Fig. 10.** Chronostratigraphic section constructed across the Cauvery deep water basin along the line BB in Fig. 1A illustrating the depositional pattern of different stratigraphic units with respect to tectonic changes. Note the ages are based on regional correlation and understandings from published literatures (Rangaraju et al., 1993; Gaina et al., 2007; Veevers, 2009; Lal et al., 2009; Bastia et al., 2010; Bastia and Radhakrishna, 2012; Nagendra and Reddy, 2017; Maitra, 2018).

governed plausibly by onlapping events as thermal bulges wane out, thus the sediments deposited primarily in relatively narrow depo-centres are surpassed by younger onlapping sequences (Figs. 2 and 3; Watts, 2001). The Palar deepwater pull-apart basin adjacent to Coromandal transform margin also has similar characteristics (Figs. 2 and 4).

A chronostratigraphic section helps to construct a relative sea level curve taking into consideration the basin set up and position (Wheeler, 1958; Rangaraju et al., 1993; Basile et al., 1998; Peters et al., 2005; Trevino et al., 2005; Raju et al., 2005; Catuneanu et al., 2009; Pigott and Radivojević, 2010; Nagendra and Reddy, 2017; Amosu and Sun, 2017). This approach has been adopted in the present study to construct a relative sea level curve from the chronostratigraphic section across the Palar - Pennar deep water pull-apart basin (Figs. 4 and 11). A pseudo well has been marked in the chronostratigraphic section (Fig. 4) of the pull-apart basin, situated in the western side of marginal ridge, along which the relative sea level curve has been constructed based on the understanding of stratal terminations (Fig. 11). It is worthwhile to understand the transform margin set up and its control on sediment depositional pattern, especially both during pre and post break-up (strike-slip movement) from the relative sea level curve (Fig. 11). The initial extension during Late Jurassic to Early Cretaceous time, typical syn-rift sedimentation happened in a grossly fluvio-lacustrine environment in the basin (Rangaraju et al., 1993; Raju et al., 2005; Nagendra and Reddy, 2017; Raju et al., 2017). Gradual sea level rise initiated towards the end of syn-rift and subsequently there was a rapid rise in early post-rift (Figs. 3 and 4; onlapping unit over the syn-rift top -M2 unconformity). Subsequent to break-up, during Early Cretaceous (M2 - M3), prograding downlapping sequence has been identified in seismic section and in the constructed chronostratigraphic section (Figs. 3 and 4;

Dasgupta, 2018a). This infers a slower rate of sea level rise likely due to strike-slip movement along the transform margin during that time. The late post-rift sequences from Mesozoic to Tertiary are affected by basin tilting and rapid subsidence. This resulted in sequential onlapping units, erosions and mass transport complex deposits (Fig. 4, Subramanian, 1987; Bastia and Radhakrishna, 2012; Dasgupta, 2018a). Thus, there is a continuous rise in sea level (Fig. 11).

With the onset of Monsoon as a result of the Himalayan orogeny (Nath, 1959; Cochran, 1990; Einsele et al., 1996; Mukherjee et al., 2015; Krishna et al., 2016; Clift, 2017), climatic controlled sedimentation prevailed in the east coast basin. The Ganga-Brahmaputra delta or the Bengal Fan started to prograde further south into lower part of Bay of Bengal, since Miocene onwards, carrying huge sediment load eroded from the Himalaya (Rao et al., 1997; Krishna et al., 2016). Accordingly, along a dip section in offshore deepwater Palar-Pennar basin, sediments thicken from Late Miocene to Recent gradually from continental slope area to the deeper abyssal plain (Figs. 2 and 4; Bastia and Radhakrishna, 2012), thereby forming a wedge. Numerous water escape structures related to polygonal faulting has been identified in this shale rich Tertiary section likely due to coeval deformation (Cartwright et al., 2003; Misra and Dasgupta, 2018a; Dasgupta and Misra, 2018; Dasgupta, 2018b). The shelf-slope instability results in submarine landslides and mass transport complexes which continue to recent times (e.g. Susanth et al., 2021b). Such rapid sedimentation at some places in the continental slope region have resulted in under-compaction and formation of mud volcano in the northern part of Palar offshore basin (Fig. 1A; Dasgupta, 2018b).

The India - Antarctic break-up along east coast of India has been documented by various authors (Veevers and Tewari, 1995; Reeves and Wit, 2000; Scotese, 2002, 2017; Kiessling et al., 2003; Gaina et al.,

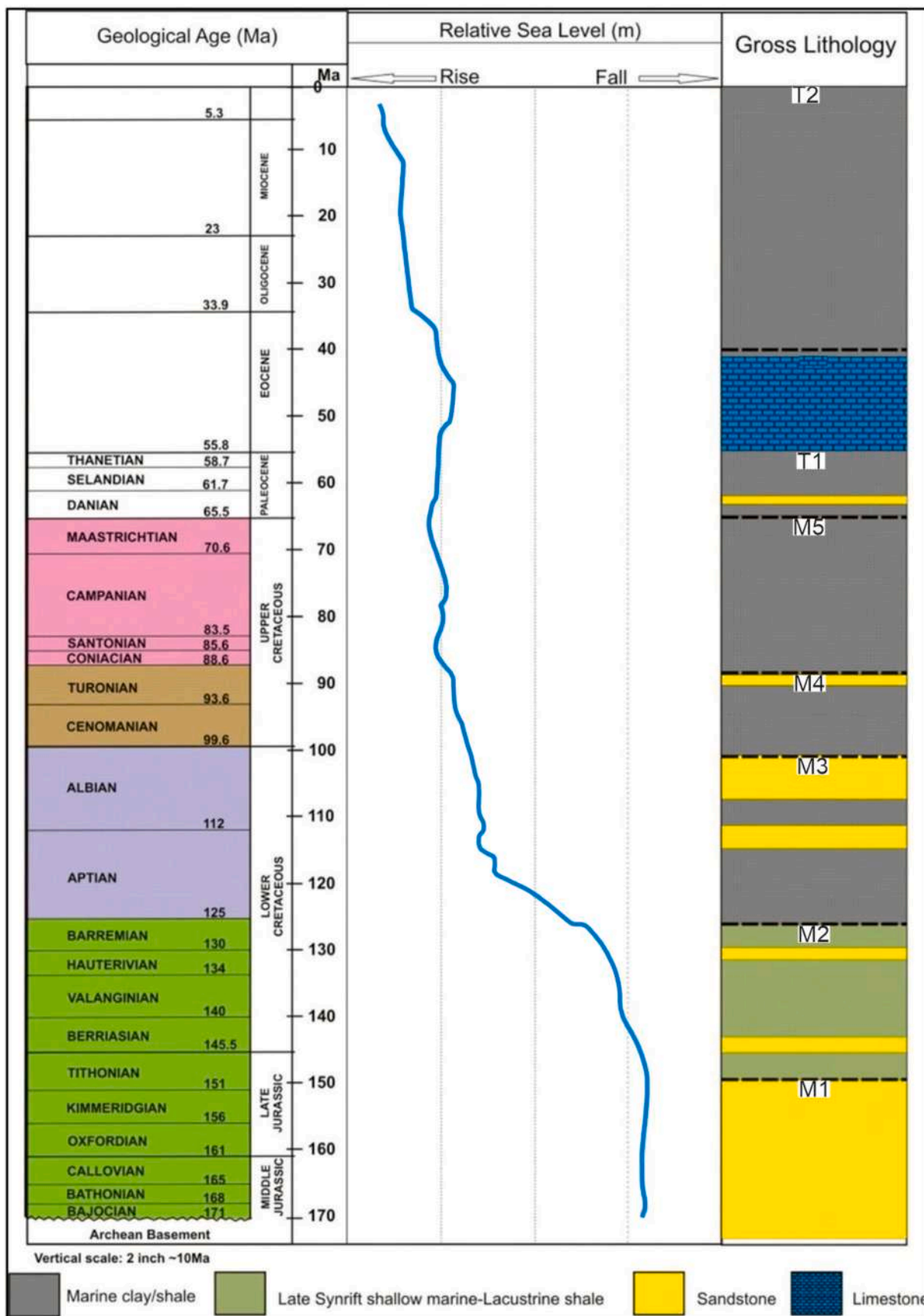
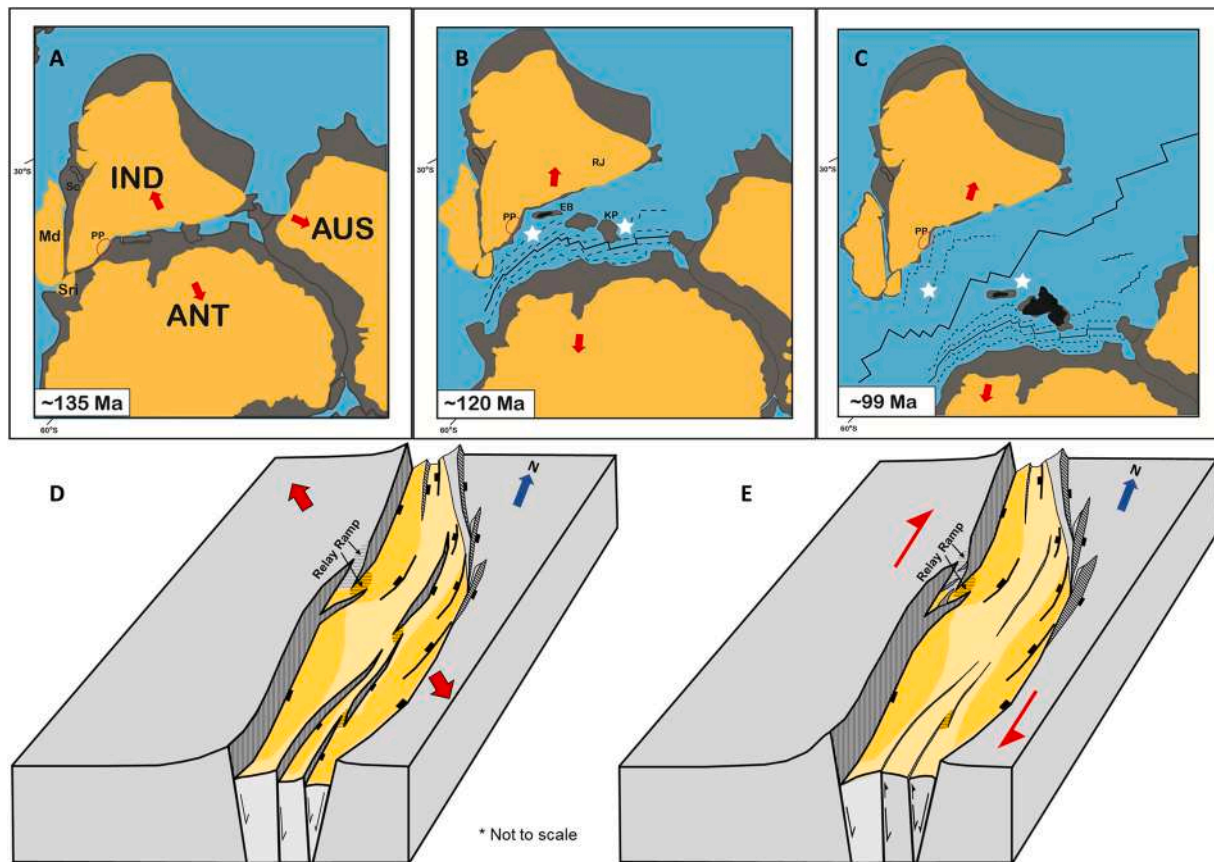


Fig. 11. Relative sea level curve constructed from the chronostratigraphic section in Fig. 4 in the offshore Palar basin along the transform margin (inputs taken from Rangaraju et al., 1993; Raju et al., 2005; Catuneanu et al., 2009; Nagendra and Reddy, 2017).



**Fig. 12.** Schematic Plate tectonic model (A, B & C) of greater India, Antarctica and Australian plate at different geological time (adapted from Reeves and Wit, 2000; Scotese, 2002; Kiessling et al., 2003; Gaina et al., 2007; Golonka, 2011; Veevers, 2012; Gibbons et al., 2013; Scotese, 2017). (A) Separation of greater India from Antarctica and Australia during Early Cretaceous (~135 Ma). (B) Initiation of separation of Elan Bank micro-continent and formation of Kerguelian hotspot activity during ~120 Ma. (C) Further northward movement of greater India from Antarctica and Elan Bank micro-continent during ~99 Ma. IND – India, ANT – Antarctica, AUS – Australia, EB – Elan Bank micro-continent, KP – Kerguelian Plateau, Md – Madagascar, Sc – Seychelles microcontinent, Sri – Sri Lanka, PP – location of Palar – Pennar basin, RJ – location of Rajmahal Traps. Red Arrows indicates the stretching direction; white star indicates the location of the hotspot activity. (D & E) Block diagram of pull-apart basin alongside a transform margin. (D) Initial basin opening due to oblique extension during rift phase- India - Antarctica separation (Late Jurassic to Early Cretaceous) creating pull-apart basins, (E) Dextral strike-slip movement along the transform margin at later stage related to separation of Antarctica followed by Elan Bank micro – continent (~Aptian). The strike-slip movement reactivated the rift faults that uplifted the basin. Presence of marginal ridges observed on the right (eastern) side of the basin. (For interpretation of the references to colour in this figure legend, the reader is referred to the Web version of this article.)

2007; Golonka, 2011; Veevers, 2012; Gibbons et al., 2013). Our work on Palar – Pennar basin of east-coast of India synthesizes the following (Fig. 12). The India – Antarctic break-up along east coast of India is a diachronous event, which initiated from Mahanadi – NE coast basin and continued through K – G up to Cauvery basin. Overall, the Palar - Pennar basin is affected by variation in stress regimes during its tectonic evolution related to India – Antarctica break-up. (a) The basin was initially under oblique extension during early rifting of India and Antarctica thereby forming pull-apart basins in Late Jurassic to Early Cretaceous Period (Ramana et al., 1994; Lal et al., 2009; Bastia et al., 2010). The Sriperumbudur Formation (Vaidyanadhan and Ramakrishnan, 2008) equivalent sediments deposited during this time in both onland and offshore sub-basins. These pull-apart sub basins and half grabens are asymmetric in nature (Vairavan, 1993; Nemčok et al., 2016; Dasgupta, 2018a; Misra and Dasgupta, 2018a). (b) This was followed by dextral strike-slip movement in which displacement shifted along the NNW cross faults during Barremian time. This strike-slip movement ultimately resulted in separation of Antarctica and subsequently the Elan Bank microcontinent along the transform margin (Bastia et al., 2010; Nemčok et al., 2013a, b; Nemčok et al., 2016). This strike-slip movement is more pronounced in the deepwater Palar basin. However its imprint is also seen in the onland from the ~NNW elongated depressions/lakes (Fig. 9). The sediment deposited during this time is equivalent to Satyavedu

Formation (Vaidyanadhan and Ramakrishnan, 2008; Basavaraju et al., 2016).

Fig. 12D and E presents a simple model to understand the two types of extension which affected the Palar pull-apart basin i.e., initial oblique extension during rifting phase (Late Jurassic to Barremian) followed by dextral strike-slip (~Barremian to Early Albian), which re-activated some of the rift faults. The Precambrian basement fabric, shear zones and lineaments guided rift propagation and subsequent reactivation (Bastia et al., 2010; Mazumder et al., 2013, 2018, 2019; Dasgupta, 2018a) in the Palar – Pennar basin. The pre-existing structures extended the basin obliquely and rifted it asymmetrically (Withjack and Jamison, 1986; Bonini et al., 2016; Dasgupta and Mukherjee, 2017, 2019).

The transform margin has a narrow shelf – slope extent associated with steep slope, thereby having short distance of transport for clastics from the shoreface and shelf to lower continental slope area (Catuneanu, 2006; Nemčok et al., 2016). Due to the high steepness of the continental slope along such margin, the sediment fairway will be governed by deep canyon cuts and straight channels (e.g. Susanth et al., 2021a) guided by the transcurrent faults. Thus, the coarser clastics deposited in the lower-mid continental slope area will normally have slope-fan geometry in the post rift sequence with a low textural maturity. The syn-rift sediments of the pull-apart basin can possess good source kitchen as well as clastic reservoir rocks. However, note that the early post rift sag

basin/sequence is missing in case of such pull-apart basin alongside transform margin due to the strike-slip movement post break-up, which reactivated earlier faults and uplift of syn-rift unit (Nemčok et al., 2016; Dasgupta, 2018a). Thus, the early post rift seal is prone to get breached. Also, the hydrocarbon migration will get affected due to such tectonic changes. A properly constructed chronostratigraphic section (Figs. 4 and 10) helps in understanding the sections having major hiatus (missing sequences), erosion and thus probable areas of insufficient seal. Hence the petroleum system elements in such offshore pull-apart basin adjacent to transform margin are very critical to understand and evaluate.

## 5. Conclusions

The entire Palar–Pennar basin evolved through different tectonic episodes with rifting guided by structural inheritance. This has its signatures both in onland terrestrial part as well as in offshore area. The key conclusions are:

- The perceived understanding from geomorphic analysis from the onland study area of Palar–Pennar basin are: (a) NW-trending lineaments most dominant, and is somewhat similar to that of offshore, (b) low sinuosity index indicating straight channels, (c) watersheds 2 and 5 are tectonically active, (d) pre-existing basement fractures have controlled the drainage pattern and recent tectonic activities, and (e) the morpho-tectonic signatures are in alignment to that of offshore Palar basin along the transform margin.
- The pull-apart basin, in the continental slope part in between the steep basement escarpment towards west and the uplifted fault block (marginal ridge) in the east, can have good source rock potential. The ~ N to NNW elongated shape of the pull-apart basin in offshore can be correlated with the ~NNW to NNE elongated lakes in the onland part. This indicates that the transtensional strike-slip movement had its impact both in continental slope as well as in the onland areas.
- A properly constructed chronostratigraphic section is extremely helpful in understanding the petroleum system in terms of reservoir presence and seal potentiality. It also helps in creating a relative sea level curve of the basin.
- In terms of hydrocarbon prospectivity, the syn-rift and early post-post rift sequence (M2 and M3) in the offshore garbens can be targeted for further study. The coarser clastic fairways (lobes and slope fans) in these sequences can be potential reservoirs. However, detail fault modelling and seal analysis from seismic data need to be done in the M2 and M3 units in order to understand the extent of fault reactivation and thus the entrapment potentiality of the plays.

## Credit author statement

**S Dasgupta**- Offshore works, writing the draft, finalization. **M Biswas**- Onshore works, writing the draft. **S Mukherjee**- Conceptualization of this multidisciplinary work, partial literature review, finalization of the draft, supervision. **R Chatterjee**-Writing and supervision.

## Declaration of competing interest

The authors declare that they have no known competing financial interests or personal relationships that could have appeared to influence the work reported in this paper.

## Acknowledgements

SDG had worked in Cauvery – Palar basins, east coast of India, as a seismic interpreter during his stay in Reliance Industries Ltd. However, in this work no data has been taken from any company/organization. CPDA grant (IIT Bombay) supported SM. Tahar Aifa (Executive Editor), reviewer Subhobroto Mazumder (ONGC) and anonymous reviewers

provided detail and critical review comments. Thanks to Mery P Ayyamperumal, Shruti Venkiteswaran, Achuthan Arivalagan, Monica Saravanan, Wan Wan and the Elsevier proofreading team for assistance.

## Appendix A. Supplementary data

Supplementary data to this article can be found online at <https://doi.org/10.1016/j.petrol.2022.110155>.

## Appendix

**DEM data specification:** Name of the Dataset: C1\_DEM\_16\_b\_2005–2014\_V3R1\_73E24N\_G43T, Theme: Terrain, Keywords: Cartosat-1, DEM, Stereo data, India, ISRO, NRSC, Used Constraints: As per NRSC Data Dissemination Policy, Purpose of creating data: Seamless DEM from IRS data, Spheroid/Datum: GCS, WGS-1984, Name of the Satellite: Cartosat-1, Sensor: PAN (2.5 m), Stereo Data.

## References

- Achyuthan, H., Thirunavukarasu, N., 2009. Quaternary stratigraphy of the Korattalayar-Coom basin, Chennai. *J. Geol. Soc. India* 73, 683–696.
- Amine, A., El Ouardi, H., Zebari, M., El Makrini, H., 2020. Active tectonics in the Moulay Idriss Massif (south Rifian ridges, NW Morocco): new insights from geomorphic indices and drainage pattern analysis. *J. Afr. Earth Sci.* 167, 103833. <https://doi.org/10.1016/j.jafrearsci.2020.103833>.
- Amosu, A., Sun, Y., 2017. WheelerLab: an Interactive Program for Sequence Stratigraphic Analysis of Seismic Sections, Outcrops and Well Sections and the Generation of Chronostratigraphic Sections and Dynamic Chronostratigraphic Sections. SoftwareX, pp. 19–24.
- Andreani, L., Stanek, K., Gloaguen, R., Krentz, O., Domínguez-González, L., 2014. DEM-based analysis of Interactions between tectonics and landscapes in the Ore Mountains and Eger rift (east Germany and NW Czech Republic). *Rem. Sens.* 6, 7971–8001. <https://doi.org/10.3390/rs6097971>.
- Anomneze, D.O., Okoro, A.U., Norbert, N.E., Akpunonu, E.O., Obiadi, I.I., Ahaneku, C.V., Okeke, G.C., 2020. Description and interpretation of fault-related sedimentation and controls on shelf-edge deltas: implication on sand transportation to the basin floor in parts of Eastern Niger Delta. *J. Petrol. Explor. Product. Technol.* 10, 1367–1388. <https://doi.org/10.1007/s13202-020-00854-z>.
- Antobreh, A.A., Faleide, J.I., Tseikalas, F., Planke, S., 2009. Rift-shear architecture and tectonic development of the Ghana margin deduced from multichannel seismic reflection and potential field data. *Mar. Petrol. Geol.* 26, 345–368.
- Asl, M.E., Faghih, A., Mukherjee, S., Soleimany, B., 2019. Style and timing of salt movement in the Persian Gulf Basin, offshore Iran: insights from halokinetic sequences adjacent to the Tonb-e-Bozorg salt diapir. *J. Struct. Geol.* 122, 116–132.
- Basavaraju, M.H., Jaiprakash, B.C., Chidambaram, L., Ayyadurai, M., 2016. Biostratigraphy and depositional environments of subsurface sediments in well Arani-A, Palar Basin, Tamil Nadu. *J. Geol. Soc. India* 88, 407–420.
- Basile, C., Mascle, J., Popoff, M., Bouillion, J.P., Mascle, G., 1993. The Ivory Coast-Ghana transform margin: a marginal ridge structure deduced from seismic data. *Tectonophysics* 222, 1–19.
- Basile, C., Masle, J., Benkheilil, J., Bouillion, J.P., 1998. Geodynamic evolution of the Côte D'Ivoire – Ghana Transform margin: an overview of Leg 159 results. *Proc. Ocean Drill. Progr. Sci. Results* 159, 101–110.
- Basile, C., Maillard, A., Patriat, M., Gaullier, V., Loncke, L., Roest, W., Mercier de L'epinay, M., Pattier, F., 2012. Structure and evolution of the Demerara Plateau, offshore French Guiana: rifting, tectonics inversion and post-rift tilting at transform-divergent margins intersection. *Tectonophysics* 591, 16–29.
- Bastia, R., Radhakrishna, M., Srinivas, T., Nayak, S., Nathaniel, D.M., Biswal, T.K., 2010. Structural and tectonic interpretation of geophysical data along the Eastern Continental Margin of India with special reference to the deepwater petroliferous basins. *J. Asian Earth Sci.* 39, 608–619.
- Bastia, R., Radhakrishna, M., 2012. Basin Evolution and Petroleum Prospectivity of the Continental Margins of India. Academic Press, Elsevier, ISBN 978-0-444-53604-4 (Developments in Petroleum Science 59).
- Bhatt, N., 2020. Geomorphology of the Indian coast: review of recent works (2016–2019). *Proc Indian Natn Sci Acad* 82, 365–368.
- Bhoj, R., 2008. Fathoming unexplored terrain. *Assoc. Petroleum Geol. Bull.* 2, 77–82.
- Biswas, S.K., 2012. Status of petroleum exploration in India. *Proc. Indian Natn. Sci. Acad.* 78, 475–494.
- Biswas, S.K., Bhasin, A.L., Ram, J., 1993. Classification of Indian sedimentary basins in the framework of plate tectonics. In: Biswas, A.K., Pandey, A., Dave, A., Maithani, A., Garg, P., Thomas, N.J. (Eds.), Proceedings of the Second Seminar on Petroliferous Basins of India, vol. 1. Indian Petroleum Publishers, Dehradun, ISBN 81-900361-0-6, pp. 1–46. East Coast, Andaman and Aasam-Arakan Basins.
- Biswas, M., Dhara, P., 2019. Correction to: Evolutionary characteristics of meander cut-off — A hydro-morphological study of the Jalangi River, West Bengal, India. *Arab. J.* 12, 739.
- Biswas, M., Paul, A., 2020. Application of geomorphic indices to address the foreland Himalayan tectonics and landform deformation-Matiali-Chalsa-Baradighi recess,

- West Bengal, India. *Quat. Int.* <https://doi.org/10.1016/j.quaint.2020.12.012> (in press).
- Biswas, M., Paul, A., Jamal, M., 2021. Tectonics and channel morpho-hydrology—a quantitative discussion based on secondary data and field investigation. In: Mukherjee, S. (Ed.), *Structural Geology and Tectonics Field Guidebook*, *ume 1*. Springer Geology, Springer, Cham. [https://doi.org/10.1007/978-3-030-60143-0\\_16](https://doi.org/10.1007/978-3-030-60143-0_16).
- Boger, S.D., Carson, C.J., Fanning, C.M., Wilson, C.J.L., 2000. Neoproterozoic deformation in the Radok Lake region of the northern Prince Charles Mountains, east Antarctica: evidence for a single protracted event. *Precambrian Res.* 104, 1–24.
- Boger, S.D., Wilson, C.J.L., Fanning, C.M., 2001. Early Paleozoic tectonism within the East Antarctic craton: the final suture between east and west Gondwana? *Geology* 29, 463–466.
- Bonini, L., Basili, R., Toscani, G., Burrato, P., Seno, S., Valensise, G., 2016. The effects of pre-existing discontinuities on the surface expression of normal faults: insights from wet-clay analog modeling. *Tectonophysics* 684, 157–175.
- Brice, J.C., 1964. Channel Patterns and Terraces of the Loup Rivers in Nebraska. Geological Survey Professional Paper 422-D, Washington, pp. D2–D41.
- Borissova, I., Coffin, M.F., Charvis, P., Operto, S., 2003. Structure and development of a microcontinent: Elean bank in the southern Indian Ocean. *Front. Res. Earth Evol.* 1, 297–303.
- Bull, W.B., McFadden, L.D., 1977. Tectonic geomorphology north and south of the Garlock fault, California. In: Doehring, D.O. (Ed.), *Geomorphology in Arid Regions. Proceedings of the Eight Annual Geomorphology Symposium*. State University of New York at Binghamton, Binghamton, NY, pp. 115–138.
- Burke, K., Sengor, C., 1989. In: Qureshy, M.N., Hinze, W.J. (Eds.), *Regional Lineaments and Continental Evolution*. Geological Society of India, Bangalore, pp. 65–73. ISSN 0016-7622.
- Carson, C.J., Boger, S.D., Fanning, C.M., Wilson, C.J.L., Thost, D., 2000. SHRIMP U–Pb geochronology from Mt Kirkby, northern Prince Charles Mountains, east Antarctica. *Antarct. Sci.* 12, 429–442.
- Cartwright, J.A., Bolton, A.J., James, D.M.D., 2003. The genesis of polygonal fault systems: a review. Geological Society London Special Publications. In: Van Rensbergen, P., Hillis, R., Maltman, A., Morley, C. (Eds.), *Subsurface Sediment Mobilization*. Special Publication Geological Society, London, pp. 223–242, 2016.
- Castellort, S., Goren, L., Willett, S., Champagnac, J., Herman, F., Braun, J., 2012. River drainage patterns in the New Zealand Alps primarily controlled by plate tectonic strain. *Nat. Geosci.* 5 (10), 744–748. <https://doi.org/10.1038/ngeo1582>.
- Catuneanu, O., 2006. Principles of Sequence Stratigraphy. Elsevier, pp. 262–278.
- Chand, S., Subrahmanyam, C., 2013. Rifting between India and Madagascar—mechanism and isostasy. *Earth Planet. Sci. Lett.* 210, 317–333.
- Chaudhuri, A., Rao, M.V., Dobriyal, J.P., Saha, G.C., Chidambaram, L., Mehta, A.K., Ramana, L.V., Murthy, K.S., 2009. Prospectivity of Cauvery basin in deep syn-rift sequences, SE India. In: AAPG Annual Convention and Exhibition, Denver, Colorado, USA, 7–10 June 2009.
- Catuneanu, O., Abreu, V., Bhattacharya, J.P., Blum, M.D., Dalrymple, R.W., Eriksson, P. G., Fielding, C.R., Fisher, W.L., Galloway, W.E., Gibling, M.R., Giles, K.A., Holbrook, J.M., Jordan, R., Kendall, C.G.C., Macurda, B., Martinsen, O.J., Miall, A. D., Neal, J.E., Nummedal, D., Pomar, L., Posamentier, H.W., Pratt, B.R., Sarg, J.F., Shanley, K.W., Steel, R.J., Strasser, A., Tucker, M.E., Winker, C., 2009. Towards the standardization of sequence stratigraphy. *Earth-Sci. Rev.* 92, 1–33.
- Chakraborty, C., Sati, G.C., Mohan, B., Bariak A. K., Bhagwani, S.S., 2012. Pennar Basin: A Potential Spot for Synrift Exploration. Society of Petroleum Geophysicists, 9th Biennial International Conference and Exposition on Petroleum Geophysics, Hyderabad. P-022.
- Chetty, T.R.K., Bhaskar Rao, Y.J., 2006. The Cauvery shear zone, southern Granulite terrain, India: a crustal-scale flower structure. *Gondwana Res.* 10, 77–85.
- Clift, P.D., 2017. Cenozoic sedimentary records of climate-tectonic coupling in the Western Himalaya. *Prog. Earth Planet. Sci.* 4, 39.
- Condie, S.A., 1993. Formation and Stability of shelf-break fronts. *J. Geophys. Res. Atmos.* 98, 12405–12416.
- Collier, J.S., Sansom, V., Ishizuka, O., Taylor, R.N., Minshull, T.N., Whitmarsh, R.B., 2008. Age of Seychelles-India break-up. *Earth Planet. Sci. Lett.* 272, 264–277.
- Cochran, J.R., 1990. Himalayan uplift, sea level, and the record of Bengal Fan sedimentation at the ODP Leg 116 sites. In: Cochran, J.R., et al. (Eds.), *Proceedings of the Ocean Drilling Program, Scientific Results*, *ume 116*. College Station, Texas, pp. 397–414.
- Cuong, N.Q., Zuchiewicz, W.A., 2001. Morphotectonic properties of the Lo river fault near Tam Dao in north Vietnam. *J. Natl. Hazards Earth Syst. Sci.* 1, 15–22.
- Dave, H.D., Mazumder, S., Pangtey, K.K.S., Tep, B., Mitra, D.S., 2013. Delineation of prospective area in Palar offshore based on analysis of natural seepage model in Cauvery offshore. In: 10th Biennial International Conference & Exposition.
- Dar, A.M., Lasitha, S., Rammiya, K., 2015. A gravity and bathymetric study in the south east continental margin of India. *J. Rem. Sens. GIS4*, 149.
- Dasgupta, et al., 2000. Southern Dharwar - southern Granulite - Palghat Cauvery shear section. In: Narula, P.L., Acharyya, S.K., Banerjee, J. (Eds.), *Seismotectonic Atlas of India and Environs*. Geological Survey of India. Charisma Printer Private Limited. Hyderabad, pp. 80–81.
- Dasgupta, S., 2018a. Pull-apart basin in the offshore Cauvery–Palar Basin, India (chapter 23). In: Misra, A.A., Mukherjee, S. (Eds.), *Atlas of Structural Geological Interpretation from Seismic Images*, first ed. Wiley Blackwell, ISBN 978-1-119-15832-5.
- Dasgupta, S., 2018b. Sedimentary deformation features produced by differential compaction and buoyancy in the offshore Palar Basin, East Coast of India (chapter 24). In: Misra, A.A., Mukherjee, S. (Eds.), *Atlas of Structural Geological Interpretation from Seismic Images*, first ed. Wiley Blackwell, ISBN 978-1-119-15832-5.
- Dasgupta, S., 2019. Implication of transfer zones in rift fault propagation: Example from Cauvery basin, Indian east coast. In: Mukherjee, S. (Ed.), *Tectonics and Structural Geology: Indian Context*. Springer Geology, Springer, Cham. [https://doi.org/10.1007/978-3-319-99341-6\\_10](https://doi.org/10.1007/978-3-319-99341-6_10).
- Dasgupta, S., 2021. A review of stratigraphy, depositional setting and paleoclimate of the different Mesozoic basins of India. In: Banerjee, S., Sarkar, S. (Eds.), *Advances in Mesozoic Stratigraphy: Multi-Proxy Approach*. Springer. [https://doi.org/10.1007/978-3-030-71370-6\\_1](https://doi.org/10.1007/978-3-030-71370-6_1).
- Dasgupta, S., Maitra, A., 2018. Transfer zone geometry in the offshore Cauvery Basin, India (chapter 21). In: Misra, A.A., Mukherjee, S. (Eds.), *Atlas of Structural Geological Interpretation from Seismic Images*, first ed. Wiley Blackwell, ISBN 978-1-119-15832-5.
- Dasgupta, S., Misra, A.A., 2018. Polygonal fault system in Late Cretaceous sediments of Cauvery deepwater Basin, India (chapter 20). In: Misra, A.A., Mukherjee, S. (Eds.), *Atlas of Structural Geological Interpretation from Seismic Images*, first ed. Wiley Blackwell, ISBN 978-1-119-15832-5.
- Dasgupta, S., Mukherjee, S., 2017. Brittle shear tectonics in a narrow continental rift: asymmetric non-volcanic Barmer basin (Rajasthan, India). *J. Geol.* 125, 561–591.
- Dasgupta, S., Mukherjee, S., 2019. Remote sensing in lineament identification: Examples from western India. In: Billi, A., Fagereng, A. (Eds.), *Problems and Solutions in Structural Geology and Tectonics. Developments in Structural Geology and Tectonics Book Series*, vol. 5. Mukherjee S. Elsevier, Series, ISBN 9780128140482, pp. 205–221. ISSN: 2542-9000.
- Dwivedi, A.K., 2016. Petroleum Exploration in India - A perspective and Endeavours. *Proc. Indian Natn. Sci. Acad.* 82, 881–903.
- Einsle, G., Ratschbacher, L., Wetzel, A., 1996. The Himalaya – Bengal Fan denudation – accumulation system during the past 20 Ma. *J. Geol.* 104, 163–184.
- Elias, Z., 2015. The neotectonic activity along the lower Khazir river by using SRTM image and geomorphic indices. *Earth Sci.* 4, 50. <https://doi.org/10.11648/j.earth.20150401.15>.
- Elias, Z., Sissakian, V., Al-Ansari, N., 2019. Assessment of the tectonic activity in north-western part of the Zagros Mountains, north-eastern Iraq by using geomorphic indices. *Geotech. Geol. Eng.* 37, 3995–4007. <https://doi.org/10.1007/s10706-019-00888-z>.
- Faghih, A., Asl, Ezati M., Mukherjee, S., Soleimany, B., 2019. Characterizing halokinesis and timing of salt movement in the Abu Musa salt diapir, Persian Gulf, offshore Iran. *Mar. Petrol. Geol.* 105, 338–352.
- Faruque, B.M., Vaz, G.G., Mohapatra, G.P., 2014. The continental shelf of eastern India, Chapter 16. In: *Continental Shelves of the World: Their Evolution during the Last Glacio-Eustatic Cycle*, Chioffi F. L., Chivas A. R., vol. 41. Geological Society of London, ISBN 9781862397057.
- Gaina, C., Muller Dietmat, R., Brown, B., Ishihara, T., Ivanov, S., 2007. Breakup and early sea floor spreading between India and Antarctica. *Geophys. J. Int.* 1–16.
- Gibbons, A.D., Whittaker, J.M., Müller, R.D., 2013. The breakup of East Gondwana: assimilating constraints from Cretaceous ocean basins around India into a best-fit tectonic model. *J. Geophys. Res. Solid Earth* 118, 808–822.
- Golonka, J., 2011. Phanerozoic palaeoenvironment and palaeolithofacies maps of the Arctic region. In: Spencer, A.M., Embry, A.F., Gautier, D.L., Stoupakova, A.V., Sørensen, K. (Eds.), *Arctic Petroleum Geology*, vol. 35. Geol. Soc. London, Memoirs, pp. 79–129 (Chapter 6).
- Gopalakrishnan, K., 2003. An overview of southern Granulite terrain, India - constraints in reconstruction of Precambrian assembly of Gondwanaland. In: Ramakrishnan, M. (Ed.), *Tectonics of Southern Granulite Terrain: Kuppam-Palani Geotranssect*. Mem Geol Soc Ind, Bangalore, ISBN 81-85867-52-6, pp. 47–78.
- Govindan, A., 2017. Discussion on Biostratigraphy and depositional environments of subsurface sediments in well Arani-A, Palar Basin, Tamil Nadu. In: Basavaraju, M.H., Jaiprakash, B.C., Chidambaram, L., Ayyadurai, M. (Eds.), *Journal of Geological Society of India*, vol. 89, pp. 99–101, 2016, 20.
- GSI, 2006. A Manual of the Geology of India, *ume 1*. Geological Survey of India Special Publication. No. 77.
- Hack, J., 1957. Studies of Longitudinal Stream Profiles in Virginia and Maryland, 294 – B. Geological Survey Professional Paper, pp. 45–95.
- Horton, R., 1945. Erosional development of streams and their drainage basins; hydrophysical approach to quantitative morphology. *Geol. Soc. Am. Bull.* 56 (3), p275. [https://doi.org/10.1130/0016-7606\(1945\)56\[275:edosat\]2.0.co;2](https://doi.org/10.1130/0016-7606(1945)56[275:edosat]2.0.co;2).
- Kailasam, L.N., 1979. Plateau uplift in peninsula India. *Tectonophysics* 61, 243–269.
- Kale, V.S., Achyuthan, H., Jaiswal, K.M., 2014. Tectonic controls upon Kaveri River drainage, cratonic Peninsular India: Inferences from longitudinal profiles, morphotectonic indices, hanging valleys and fluvial records. *Geomorphology* 227, 153–165.
- Keller, E.A., Pinter, N., 2002. Active Tectonics: Earthquakes, Uplift, and Landscape, second ed. Prentice Hall, New Jersey, pp. 1–362.
- Kiessling, W., Flügel, E., Golonka, J., 2003. Patterns of Phanerozoic carbonate platform sedimentation. *Lethaia* 36, 195–226. Oslo. ISSN 0024 – 1164.
- Krishna, K.S., Michael, Laju, Bhattacharyya, R., Majumdar, T.J., 2009. Geoid and gravity anomaly data of conjugate regions of Bay of Bengal and Enderby Basin – new constraints on breakup and early spreading history between India and Antarctica. *J. Geophys. Res.* 114, B03102. <https://doi.org/10.1029/2008JB005808>.
- Krishna, K.S., Ismaiel, Md, Srinivas, K., Rao, D.G., Mishra, J., Saha, D., 2016. Sediment pathways and emergence of Himalayan source material in the Bay of Bengal. *Curr. Sci.* 110, 363–372. <https://doi.org/10.18520/cs/v110/i3/363-372>.
- Lal, N.K., Siwal, A., A, Kaul, A.K., 2009. Evolution of east coast of India – a Plate tectonic reconstruction. *J. Geol. Soc. India* 73, 249–260.
- Lee, C., Tsai, L.L., 2009. A quantitative analysis for geomorphic indices of longitudinal river profile: a case study of the Choushui River, Central Taiwan. *Environ. Earth Sci.* 59, 1549–1558.

- Mahadevan, T.M., 1994. Deep continental structure of India: a review. *Geol. Soc. India. Mem.* 28. Bangalore. pp. 38, 40, 41, 50, 82, 146.152, 433, 451, ISBN - 81- 85867 - 06 -2.
- Mahadevan, T.M., 2003. Geological Evolution of South Indian Shield - Constrains on Modelling. In: Ramakrishnan, M (Ed.), *Tectonics of Southern Granulite Terrain: Kuppam-Palani Geotranssect. Mem. Geol. Soc. Ind., Bangalore*, pp. 25–46. ISBN 81-85867-52-6.
- Mahmood, S., Gloaguen, R., 2012. Appraisal of active tectonics in Hindu Kush: insights from DEM derived geomorphic indices and drainage analysis. *Geosci. Front.* 3, 407–428.
- Maitra, A., 2018. Synrift grabens and inversion in the Cauvery offshore basin on the east Coast of India (Chapter 22). In: Misra, A.A., Mukherjee, S. (Eds.), *Atlas of Structural Geological Interpretation from Seismic Images*, first ed. Wiley Blackwell, ISBN 978-1-119-15832-5.
- Matin, A., 2014. Tectonics in the Cuddapah fold–thrust belt in the Indian shield, Andhra Pradesh, India and its implication on the crustal amalgamation of India and Rayner craton of Antarctica during Neoproterozoic orogenesis. *Int. J. Earth Sci.* 103, 7–22.
- Mazumder, S., Pangtey, K.K.S., Mitra, D.S., 2013. Delineation of a Possible Subsurface Ridge in Onshore Palar Basin Based on Morphotectonic Studies and its Implications. 10th Biennial International Conference & Exposition, pp. 1–6.
- Mazumder, S., Tep, B., Pangtey, K.K.S., et al., 2019. Basement/Tectonics and shear zones in Cauvery basin: implications in hydrocarbon exploration. In: Mukherjee, S. (Ed.), *Tectonics and Structural Geology: Indian Context*. Springer International Publishing AG, Cham.
- Mazumder, S., Tep, B., Pangtey, K.K.S., Mitra, D.S., 2018. A morphotectonic based approach to derive tectonic framework and possible areas of hydrocarbon accumulation in onshore Palar basin. *ONGC Bulletin* 48, 112–123.
- Mazumder, R., Eriksson, P.G., 2015. Precambrian basins of India: stratigraphic and tectonic context. *Geol. Soc. Londn. Mem.* 43, 231–254. <https://doi.org/10.1144/M43.16>.
- Mezger, K., Cosca, M.A., 1999. The thermal history of the Eastern Ghats belt (India) as revealed by U–Pb and 40Ar/39Ar dating of metamorphic and magmatic minerals: implications for the SWEAT correlation. *Precambrian Res.* 94, 251–271.
- Miall, A.D., 1977. A review of the braided river depositional environment. *Earth Sci. Rev.* 13, 1–62.
- Miall, A.D., 1997. *The Geology of Stratigraphic Sequences*. Springer, pp. 271–384.
- Misra, A.A., Bhattacharya, G., Mukherjee, S., Bose, N., 2014. Near N–S paleo-extension in the western Deccan region, India: Does it link strike-slip tectonics with India–Seychelles rifting? *Int. J. Earth Sci.* 103, 1645–1680.
- Misra, A.A., Dasgupta, S., 2018a. Transform margin in the Cauvery Basin, Indian east coast passive margin (chapter 46). In: Misra, A.A., Mukherjee, S. (Eds.), *Atlas of Structural Geological Interpretation from Seismic Images*, first ed. Wiley Blackwell, ISBN 978-1-119-15832-5.
- Misra, A.A., Dasgupta, S., 2018b. Shallow Detachment along a transform margin in Cauvery basin, India (chapter 18). In: Misra, A.A., Mukherjee, S. (Eds.), *Atlas of Structural Geological Interpretation from Seismic Images*, first ed. Wiley Blackwell, ISBN 978-1-119-15832-5.
- Misra, A.A., Mukherjee, S., 2018. *Atlas of Structural Geological Interpretation from Seismic Images*. Wiley Blackwell, ISBN 978-1-119-15832-5.
- Morisawa, M., 1985. *Rivers. Longman*, ISBN 0-582-48982-2, pp. 1–222. Price: £12.95.
- Mukherjee, S., Carosi, R., van der Beek, P.A., Mukherjee, B.K., Robinson, D.M., 2015. *Tectonics of the Himalaya: an Introduction*, vol. 412. Geological Society, London, Special Publications, pp. 1–3.
- Mukherjee, S., Goswami, S., Mukherjee, A., 2019. Structures and their tectonic implications of the southern part of Cuddapah basin, Andhra Pradesh, India. *Iranian Journal of Science and Technology Transaction: A: Science* 43, 489–505.
- Nagaraja Rao, B.K., Rajurkar, S.T., Ramalingaswamy, G., Ravindra Babu, B., 1987. Stratigraphy, structure and evolution of the Cuddapah basin. In: Radhakrishna, B.P. (Ed.), *Purana Basins of Peninsular India, Middle to Late Proterozoic*, vol. 6. Geological Society of India, Bangalore, Memoirs, pp. 33–86.
- Nabavi, S.T., Alavi, S.A., Jabarabadi, H.J., 2019. The Dinevar transtensional pull-apart basin, NW Zagros Mountains, Iran: a geological study and comparison to 2D finite element elastic models. *Int. J. Earth Sci.* 108, 329–346. <https://doi.org/10.1007/s00531-018-1656-0>.
- Nagendra, R., Reddy, A.N., 2017. Major geologic events of the Cauvery Basin, India and their correlation with global signatures - a review. *J. Palaeogeogr.* 6, 69–83.
- Nath, J.S., 1959. *Himalayan Orogeny and Sedimentary Cycles, Symposium on Tectonic*. <https://www.ias.ac.in/public/Volumes/secb/053/03/0111-0124.pdf>.
- Naqvi, S.M., Rogers, J.J.W., 1987. *Precambrian Geology of India*. Oxford University Press, New York.
- Nemčok, M., Stuart, C., Rosendahl, B.R., Welker, C., Smith, S., Sheya, C., Sinha, S.T., Choudhuri, M., Allen, R., Reeves, C., Sharma, S.P., Venkatraman, S., Sinha, N., 2013a. Continental Break-Up Mechanism; Lessons from Intermediate- and Fast-Extension Settings, vol. 369. Geological Society London, Special Publication, pp. 373–401.
- Nemčok, M., Sinha, S.T., Stuart, C.J., Welker, C., Choudhuri, M., Sharma, S.P., Misra, A.A., Sinha, N., Venkatraman, S., 2013b. East Indian margin evolution and crustal architecture: integration of deep reflection seismic interpretation and gravity modeling. *Geol. Soc. Londn. Special Publ.* 369, 477–496.
- Nemčok, M., Rybár, S., Sinha, S.T., Hermeston, S.A., Ledvényiová, L., 2016. Transform Margins: Development, Controls and Petroleum Systems – an Introduction, vol. 431. Geological Society, London, Special Publications, pp. 1–38.
- Pareta, K., Pareta, U., 2011. Quantitative morphometric analysis of a watershed of Yamuna basin, India using ASTER (DEM) data and GIS. *Int. J. Geomatics Geosci.* 2.
- Paul, A., Biswas, M., 2019. Changes in riverbed terrain and its impact on flood propagation – a case study of River Jayanti, West Bengal, India. *Geomatics, Nat. Hazards Risk* 10, 1928–1947. <https://doi.org/10.1080/19475705.2019.1650124>.
- Peters, J., Mahanti, S., Singh, S.K., 2005. *Sedimentary basins of India*. In: Raju, D.S.N., Peters, J., Shanker, R., Kumar, G. (Eds.), *An Overview of Litho-Bio-Chemo-Sequence Stratigraphy and Sea Level Changes of Indian Sedimentary Basins*, vol. 1. APG Special Publication, pp. 8–9.
- Pigott, J.D., Radičević, D., 2010. Seismic stratigraphy based Chronostratigraphy (SSBC) of the Serbian Banat region of the Pannonian basin. *Cent. Eur. J. Geosci.* 2, 481–500.
- Posamentier, H.W., Walker, R.G., 2006. Deepwater turbidites and submarine fans. In: Posamentier, H.W., Walker, R.G. (Eds.), *Facies Models Revisited, Special Publication*, vol. 84. Society for Sedimentary Geology (SEPM), pp. 397–520.
- Powell, C. McA., Pisarevsky, S.A., 2002. Late Neoproterozoic assembly of east Gondwana. *Geology* 30, 3–6.
- Prakash, K., Singh, S., Mohanty, T., Chaubey, K., Singh, C., 2017. Morphometric assessment of Gomati river basin, middle Ganga plain, Uttar Pradesh, North India. *Spatial Information Research* 25, 449–458. <https://doi.org/10.1007/s41324-017-0110-x>.
- Rai, P.K., Mohan, K., Mishra, S., et al., 2017. A GIS-based approach in drainage morphometric analysis of Kanhar River Basin, India. *Appl. Water Sci.* 7, 217–232. <https://doi.org/10.1007/s13201-014-0238-y>.
- Rajaniikanth, A., Agarwal, A., Stephen, A., 2010. An integrated inquiry of early Cretaceous flora, Palar basin, India. *Phytomorphology* 60, 21–28.
- Raju, D.S.N., Jaiprakash, B.C., Ravindran, C.N., Kalyanasunder, R., Ramesh, P., 2005. The magnitude of hiatus and sea level changes across K/T Boundary in Cauvery and Krishna-Godavari Basins. In: Raju, D.S.N., Peters, J., Shanker, R., Kumar, G. (Eds.), *Indian Association of Petroleum Geologists*, pp. 104–113.
- Raju, D.S.N., Reddy, A.N., Jaiprakash, B.C., Gilbert, H., Sangwar, D.P., 2017. Age and paleoenvironmental evolution of the syn-rift fill sediments in east coast basins of India. *ONGC Bulletin* 52, 127–148.
- Ramakrishnan, M., 2003. Craton-mobile belt Relations in southern Granulite terrain. In: Ramakrishnan, M. (Ed.), *Tectonics of Southern Granulite Terrain: Kuppam-Palani Geotranssect. Mem. Geol. Soc. Ind, Bangalore*, ISBN 81-85867-52-6, pp. 1–24.
- Ramana, M.V., Nair, R.R., Sarma, K.V.L.N.S., Ramprasada, T., Krishna, K.S., D'cruz, Maria, Subramanyam, C., Paul, J., Subramanyam, A.S., Chandra Shekhar, D. V., 1994. Mesozoic anomalies in the bay of Bengal. *Earth Planet Sci. Lett.* 121, 469–475 (s).
- Ramasamy, S.M., Kumanan, C.J., Selvakumar, R., Saravanavel, J., 2011. Remote sensing revealed drainage anomalies and related tectonics of South India. *Tectonophysics* 501, 41–51.
- Ramírez-Herrera, M.T., 1998. Geomorphic assessment of active tectonics in the Acambay Graben, Mexican volcanic belt. *Earth Surf. Process. Landforms* 23, 317–332.
- Rangaraju, M.K., Aggarwal, A., Prabhakar, K.N., 1993. Tectono-stratigraphy, structural styles, evolutionary model and hydrocarbon prospects of Cauvery and Palar Basins, India. 1. *Indian Petroleum Publishers, Dehradun, India*, pp. 331–354.
- Rao, D.G., Krishna, K.S., Sar, D., 1997. Crustal evolution and sedimentation history of the bay of Bengal since the Cretaceous. *J. Geophys. Res.* 102 (17), 747–768.
- Ravnås, R., Steel, R.J., 1998. Architecture of marine rift basin successions. *AAPG (Am. Assoc. Pet. Geol.) Bull.* 82, 110–146.
- Reeves, C., Wit, M., 2000. Making ends meet in Gondwana: retracing the transforms of the Indian Ocean and reconnecting continental shear zones. *Terra. Nova* 12, 272–280.
- Reeves, C.V., 2013. The global tectonics of the Indian Ocean and its relevance to India's western margin. *J. Geophys.* 34, 87–94.
- Resmi, M.R., Achyuthan, H., Jaiswal, M.K., 2016. Middle to late Holocene paleochannels and migration of the Palar river, Tamil Nadu: implications of neotectonic activity. *Quat. Int.* 443, 211–222.
- Resmi, M.R., Achyuthan, H., 2018. Lower Palar river sediments, southern peninsular, India: Geochemistry, source-area weathering, provenance and tectonic setting. *J. Geol. Soc. India* 92, 83–91.
- Resmi, M.R., Babeesh, C., Hema Achyuthan, H., 2019. Quantitative analysis of the drainage and morphometric characteristics of the Palar River basin, Southern Peninsular India; using bAd calculator (bearing azimuth and drainage) and GIS. *Geol. Ecol. Landscapes* 3 (4), 295–307. <https://doi.org/10.1080/24749508.2018.1563750>.
- Sastri, V.V., Sinha, R.N., Singh, G., Murti, K.V.S., 1973. Stratigraphy and Tectonics of sedimentary basins on east coast of Peninsular India. *Bull. AAPG* 57, 655–678.
- Saxena, V.M., Chakraborty, C., Sati, G.C., Mohan, B., Bariak, A.K., Bhagwani, S.S., 2012. Pennar Basin: A Potential Spot for Synrift Exploration. 9th Biennial International Conference & Exposition on Petroleum Geophysics, pp. 1–16.
- Sajadian, M., Pourkermani, M., QorasHi, M., Moghaddas, N.H., 2015. The analysis of transverse Topographic symmetry factor (T index) in the Chekene-Mazavand, north east Iran. *Open J. Geol.* 5, 809–820. <https://doi.org/10.4236/ojg.2015.511069>.
- Schumm, S.A., Khan, H.R., 1972. Experimental study of channel patterns. *Nature* 223, 407–409.
- Schumm, S.A., 1956. The evolution of drainage systems and slopes in bad lands at Perth, Amboi, New Jersey. *Geol. Soc. Am. Bull.* 67, 597–646.
- Scotese, C.R., 2002. *PALEOMAP Project*. <http://www.scotese.com>. (Accessed 12 January 2021).
- Scotese, C.R., 2017. *Atlas of Oceans & Continents: Plate Tectonics, 1.5 by – Today, PALEOMAP Project Report 112117A*.
- Silva, P.G., Goy, J.L., Zazo, C., Azcárate, T., 2003. Fault-generated mountain fronts in southeast Spain. Geomorphologic assessment of tectonic and seismic activity. *Geomorphology* 50, 203–225.

- Sinha, S.T., Nemčok, M., Choudhuri, M., Misra, A.A., Sharma, S.P., Sinha, N., Venkatraman, S., 2010. The Crustal Architecture and Continental Break up of East India Passive Margin: an Integrated Study of Deep Reflection Seismic Interpretation and Gravity Modeling. Search and Discovery Article #40611.
- Storey, M., Mahoney, J.J., Saunders, A.D., Duncan, R.A., Kelley, S.P., Coffin, M.F., 1995. Timing of hot-spot related volcanism and the breakup of Madagascar and India. *Science* 267, 852–855.
- Smith, G., 1935. The relative relief of Ohio. *Geogr. Rev.* 25, 272–284. <https://doi.org/10.2307/209602>.
- Strahler, A.N., 1952. Hypsometric (area-altitude) analysis of erosional topography. *Geol. Soc. Am. Bull.* 63, 1117–1142.
- Subbarao, K.V., Chandrasekharam, D., Navaneethakrishnan, Hooper P.R., 1994. Stratigraphy and structure of parts of the central Deccan Province: eruptive models. In: Subbarao, K.V. (Ed.), *Volcanism*. Wiley, New Delhi, pp. 321–332.
- Subramanian, K.S., 1987. Possible cause of Easterly tilt of the Southern part of India. *J. Geol. Soc. India* 29, 362–363.
- Subrahmanyam, V., Subrahmanyam, A.S., Murthy, K.S.R., Murty, G.P.S., Sarma, K.V.L.N.S., Suneeta Rani, P., Anuradha, A., 2006. Precambrian mega lineaments across the Indian sub-continent - preliminary evidence from offshore magnetic data. *Curr. Sci.* 90, 578–581.
- Susanth, S., John Kurian, P., Bijesh, C.M., Twinkle, D., Tyagi, A., Rajan, S., 2021a. Controls on the evolution of submarine canyons in steep continental slopes: geomorphological insights from Palar Basin, south eastern margin of India. *Geo Mar. Lett.* 41, 14.
- Susanth, S., John Kurian, P., Bijesh, C.M., Twinkle, D., Bijesh, C.M., Tyagi, A., 2021b. Potential submarine landslide zones off Chennai, southeast continental margin of India. *Reg. Stud. Mar. Sci.* 45, 101832.
- Takieh, E., Ghorashi, M., Rezaie, F., 2015. The transverse topographic symmetry factor of Darakeh stream in the north Tehran, Iran. *Open J. Geol.* 5, 770–779. <https://doi.org/10.4236/ojg.2015.511066>.
- Trevino, R.H., Brown Jr., L.F., Loucks, R.G., Hammes, U., 2005. “Wheeler diagrams”: a useful exploration tool in the Gulf of Mexico. *Gulf Coast Assoc. of Geol. Soc. Trans.* 55, 830–834.
- Tripathy, V., Satyapal, Mitra S.K., Sessa Sai, V.V., 2019. Fold-Thrust belt architecture and structural evolution of the northern part of the Nallamalai fold belt, Cuddapah basin, Andhra Pradesh, India. In: Mukherjee, S. (Ed.), *Tectonics and Structural Geology: Indian Context*. Springer Geology, pp. 219–252. [https://doi.org/10.1007/978-3-319-99341-6\\_7](https://doi.org/10.1007/978-3-319-99341-6_7).
- Tripathy, V., Saha, D., 2013. Plate margin paleostress variations and intracontinental deformations in the evolution of the Cuddapah basin through Proterozoic. *Precambrian Res.* 235, 107–130.
- Twinkle, D., Srinivasa Rao, G., Radhakrishna, M., Murthy, K.S.R., 2016. Crustal structure and rift tectonics across the Cauvery–Palar basin, Eastern Continental Margin of India based on seismic and potential field modelling. *J. Earth Syst. Sci.* 125 (No. 2), 329–342.
- URL 1: <https://www.offshore-mag.com/drilling-completion/article/16776985/reliance-hits-with-first-cauverypalar-basin-well> (Accessed on 2nd Nov 2021).
- URL 2: <https://www.dghindia.gov.in/> (Accessed on 2nd Nov 2021).
- URL 3: <https://www.thehindu.com/news/national/ongc-begins-drilling-in-palar-basin> (Accessed on 31-Oct-2021).
- Vaidyanadhan, R., Ramakrishnan, M., 2008. *Geology of India*, vol. 2. Geol Society of India, Bangalore, pp. 917–918.
- Vail, P.R., Mitchum Jr., R.M., Thompson, S., 1977. *Seismic Stratigraphy and Global Changes in Sea Level, Part Four: Global Cycles of Relative Changes of Sea Level*, vol. 26. AAPG Memoir, pp. 83–98.
- Vail, P.R., 1987. Seismic stratigraphy interpretation procedure. In: Bally, A.W. (Ed.), *Atlas of Seismic Stratigraphy: AAPG Studies in Geology* 1, pp. 1–10.
- Vairavan, V., 1993. Tectonic history and hydrocarbon prospect of Palar and Pennar basins. In: Biswas, A.K., Pandey, A., Dave, A., Maithani, A., Garg, P., Thomas, N.J. (Eds.), *Proceedings of the Second Seminar on Petroliferous Basins of India*, vol. 1. Indian Petroleum Publishers, Dehradun, ISBN 81-900361-0-6, pp. 389–396. East Coast, Andaman and Aasam-Arakan Basins.
- Varadarajan, K., Ganju, J.L., 1989. In: Qureshy, M.N., Hinze, W.J. (Eds.), *Lineament Analysis of Coastal Belt of Peninsular India*. Geological Society of India, Bangalore, pp. 35–42. ISSN 0016-7622.
- Veevers, J.J., 2009. Palinspastic (pre-rift and -drift) fit of India and conjugate Antarctica and geological connections across the suture. *Gondwana Res.* 16, 90–108.
- Veevers, J.J., 2012. Reconstructions before rifting and drifting reveal the geological connections between Antarctica and its conjugates in Gondwanaland. *Earth Sci. Rev.* 111, 249–318.
- Veevers, J.J., Tewari, R.C., 1995. Gondwana Master Basin of Peninsular India between Tethys and the Interior of the Gondwanaland Province of Pangea, vol. 187. Geological Society of America Memoir, p. 72.
- Venkatakrishnan, R., Dotiwala, F.E., 1987. The Cuddapah salient: a tectonic model for the Cuddapah Basin, India, based on Landsat image interpretation. *Tectonophysics* 136, 237–253.
- Watts, A.B., 2001. *Isostasy and Flexure of the Lithosphere*. Department of Earth Sciences. Cambridge University Press, Oxford University, pp. 336–370.
- Withjack, M.O., Jamison, W.R., 1986. Deformation produced by oblique rifting. *Tectonophysics* 126, 99–124.
- Widdowson, M., 1997. Tertiary palaeosurfaces of the SW Deccan, Western India: implications for passive margin uplift. In: Widdowson, M. (Ed.), *Palaeosurfaces: Recognition, Reconstruction and Palaeoenvironmental Interpretation*, vol. 120. Geological Society, London, Special Publications, pp. 221–248.
- Wheeler, H.E., 1958. Time-stratigraphy. *AAPG Bull.* 42, 1045–1063.
- Whipple, K., Wobus, C., Crosby, B., Kirby, E., Sheenan, D., 2007. New Tools for Quantitative Geomorphology: Extracting and Interpretation of Stream Profiles from Digital Topographic Data. *GSA Annual Meeting*, Boulder, USA.
- Wobus, C., Whipple, K., Kirby, E., Snyder, N., Johnson, J., Spyropoulou, K., Crosby, B., Sheehan, D., 2006. Tectonics from topography: procedures, promise, and pitfalls. In: *Tectonics, Climate, and Landscape Evolution*, vol. 398. Special Paper - Geological Society of America, pp. 55–74.
- Wolosiewicz, B., 2018. The influence of the deep seated geological structures on the landscape morphology of the Dunajec River catchment area, Central Carpathians, Poland and Slovakia. *Contemp. Trends Geosci.* 7, 21–47. <https://doi.org/10.2478/ctg-2018-0002>.
- Zachariah, A.J., Gawthorpe, R., Dreyer, T., 2009. Evolution and strike variability of early post-rift deep-marine depositional systems: lower to mid-Cretaceous, north Viking graben, Norwegian north sea. *Sediment. Geol.* 220, 60–76.
- Ziyad, E., 2014. Relationship between tectonic activity, fluvial system and river morphology in the Dohuk catchment, Iraqi Kurdistan. *Geomorphol.: Relief, Process. Environ.* 20, 91–100. <https://doi.org/10.4000/geomorphologie.10539>.